KERNFORSCHUNGSZENTRUM

KARLSRUHE
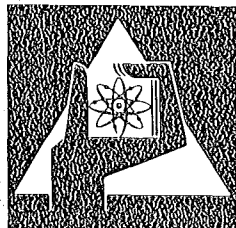
Vapour Pressure Measurements to 7000 K and Equation of State of Oxide Fuels for Fast Reactor Safety Analysis

H. G. Bogensberger, E. A. Fischer
P. G. Berrie, P. R. Kinsman, R. W. Ohse
(Europäisches Institut für Transurane)

Vapour Pressure Measurements to 7000 K and Equation

of State of Oxide Fuels for Fast

Reactor Safety Analysis

by

H.G. Bogensberger, E.A. Fischer

P.G. Berrie*, P.R. Kinsman*, R.W. Ohse*

*

Europäisches Institut für Transurane

Part I: Extension of Vapour Pressure Measurements of Nuclear Fuels (U, Pu)O_2 and UO_2 to 7ooo K

Abstract

A new high-energy laser technique, including fast temperature recording in the microsecond range, was developed for measuring the vapour pressure of fast breeder uranium-plutonium oxide fuels up to 7000 K. In the ternary system, the pressure of uranium-plutonium oxide above its melting point was determined to be log p (atm) = 7.966 - (28137/T), yielding a high-temperature heat of evaporation of ΔH_{evap} = 128.7 kcal/mol. Measurement of the UO_2 partial pressure over the solid gave log p (atm) = 9.365 - (32436/T), resulting in a heat of sublimation of ΔH_{sub} = 148.4 kcal/mol. The difference of these heats yields the heat of fusion ΔH_f = 19.7 kcal/mol, which is in good agreement with the literature value of 19.4 kcal/mol. In the binary UO_2 system, the pressure above the melting point was determined to be log p (atm) = 7.7 - (27900/T), giving a heat of evaporation of ΔH_{evap} = 127.6 kcal/mol. An assessment of literature data for below the melting point yielded log p (atm) = 8.846 - (31506/T), and a heat of sublimation of ΔH_{sub} = 144.1 kcal/mol. The resulting heat of fusion, ΔH_f = 16.5 kcal/mol, is only slightly below the published value of ΔH_f = 17.7 kcal/mol.

Teil I: Ausdehnung von Dampfdruckmessungen an Kernbrennstoffen (U, Pu)O_2 und UO_2 bis 7ooo K

Zusammenfassung

Es wurde eine neue Hochenergie-Lasertechnik, einschließlich schneller Temperaturaufzeichnung im Mikrosekundenbereich, zur Messung des Dampfdrucks schneller oxidischer Uran-Plutonium Brüter-Brennstoffe bis 7000 K entwickelt. Die Messungen am ternären System der Uran Plutonium Oxide ergaben oberhalb des Schmelzpunktes einen Dampfdruck von log p (atm) = 7.966 - 28137/T. Hieraus folgt eine Verdampfungsenthalpie von ΔH_{Verd} = 128,7 kcal/Mol. Die Messung des UO_2 Partialdrucks über der festen Phase ergab log p (atm) = 9,365 - 32436/T mit einer Sublimationsenthalpie von ΔH_{Sub} = 148,4 kcal/Mol. Die Differenz beider Enthalpien ergibt eine Schmelzwärme von ΔH_f = 19,7 kcal/Mol, welche gut mit dem Literaturwert von 19,4 kcal/Mol übereinstimmt. Im binären UO_2 System wurde der Dampfdruck oberhalb des Schmelzpunktes zu log p (atm) = 7,7 - 27900/T mit einer Verdampfungsenthalpie von ΔH_{Verd} = 127,6 kcal/Mol bestimmt. Eine Auswertung der Literaturdaten unterhalb des Schmelzpunktes ergab log p (atm) = 8,846 - 31506/T mit einer Sublimationsenthalpie von ΔH_{Sub} = 144,1 kcal/Mol. Die hieraus resultierende Schmelzwärme von ΔH_f = 16,5 kcal/Mol liegt nur wenig unter dem publizierten Wert von ΔH_f = 17,7 kcal/Mol.

Part II: Critical Assessment of Equation of State Data for UO_2

Abstract

A new equation of state for UO_2 has been derived using the theory of significant liquid structures, which predicts a critical temperature of 7560 K, a critical pressure of 1210 atm, and a critical density of 1.66 g/cm^3. The resulting critical compressibility of 0.316 is in good agreement with the values predicted by the theory of corresponding states. Consistency between literature data on enthalpy of solid UO_2, recent vapour pressure measurements over liquid UO_2, and the pressure data over solid UO_2 could only be obtained by the inclusion of an electronic exitation term in the gaseous partition function. A new set of free energy functions for gaseous and solid UO_2 is presented.

Teil II: Kritsche Auswertung von Zustandsdaten für UO_2

Zusammenfassung

Eine neue Zustandsgleichung für UO_2 wurde aus der Theorie der signifikanten Strukturen der Flüssigkeit (theory of significant liquid structures) abgeleitet. Die Theorie ergibt eine kritische Temperatur von 7560 K, einen kritischen Druck von 1210 atm, und eine kritische Dichte von 1,66 g/cm^3. Die resultierende kritische Kompressibilität stimmt gut mit dem Wert überein, der aus der Theorie der korrespondierenden Zustände folgt. Die Literaturdaten für die Enthalpie des festen UO_2, die kürzlich durchgeführten Dampfdruckmessungen (Teil 1) über flüssigem UO_2 und die Dampfdruckdaten über festem UO_2 sind nur konsistent, wenn man einen Term für Elektronenanregung in der Zustandssumme für UO_2-Gas einführt. Neue Daten für die freien Energiefunktionen von festem und gasförmigem UO_2 werden angegeben.

Table of Contents

Part I: Extension of Vapour Pressure Measurements of Nuclear
        Fuels (U, Pu)O_2 and UO_2 to 7000 K

Part II: Critical Assessment of Equation of State Data for UO_2

Part I: Extension of Vapour Pressure Measurements of Nuclear Fuels $(U, Pu)O_2$ and UO_2 to 7000 K

R.W. Ohse, P.G. Berrie
Europäisches Institut für Transurane

H.G. Bogensberger, E.A. Fischer
Institut für Neutronenphysik und Reaktortechnik

1. Introduction

In view of the projected increase in nuclear power plants, reactor safety has become a subject of major importance. One of the fields attracting the most attention is the estimation of the energy yield in a reactor core melt down accident. For complete analysis of such a hypothetical accident it is necessary to know the equation of state of the irradiated fuel at temperatures up to 5000°K or more, since the vapour pressure is the ultimate shut-down mechanism. Previous analyses have depended upon the extrapolation of low-temperature data and the results of theoretical models. Experimental measurements of vapour pressure up to 5000°K are urgently required because of the large extrapolation of data and disagreement between the various approaches. The object of this project is to extend previous measurements up to 5000°K by the development of a new technique.

2. Vapour pressure over the solid phase

The vapour pressure measurements of the three systems U-O /1-7/, Pu-O /8-12/ and U-Pu-O /13-14/ are presented in Figs.1,2 and 3. The methods used have been Knudsen effusion with target collection, mass spectrometric ion intensity measurements and the transpiration technique.

Under vacuum the uranium dioxide tends to become only slightly substoichiometric at high temperatures when approaching the congruently evaporating composition, as shown by Ohse /3,15/ and Tetenbaum et al /6/. The Pu-O and U-Pu-O systems are both characterized by a wide substoichiometric range. The high temperature single phase region of the Pu-O system runs from O/Pu = 2.00 to 1.60, showing a bi-variant behaviour in agreement with the phase rule, where the pressure is a function of both temperature and composition.

The total pressure above all three systems passes through a minimum, which in the case of the binary systems Pu-O and U-O occurs at the true congruently evaporating compositions /8,12,6/ where $(O/M)_s = (O/M)_g$. The minimum in the U-O system is near the stoichiometric composition /6/, whereas in the Pu-O system this minimum was found in the composition range O/Pu = 1.83 to 1.87 /9,12/, both depending on temperature. In the ternary system a congruently evaporating composition does not exist. The composition of the condensed phase will go on changing towards the uranium rich side. A
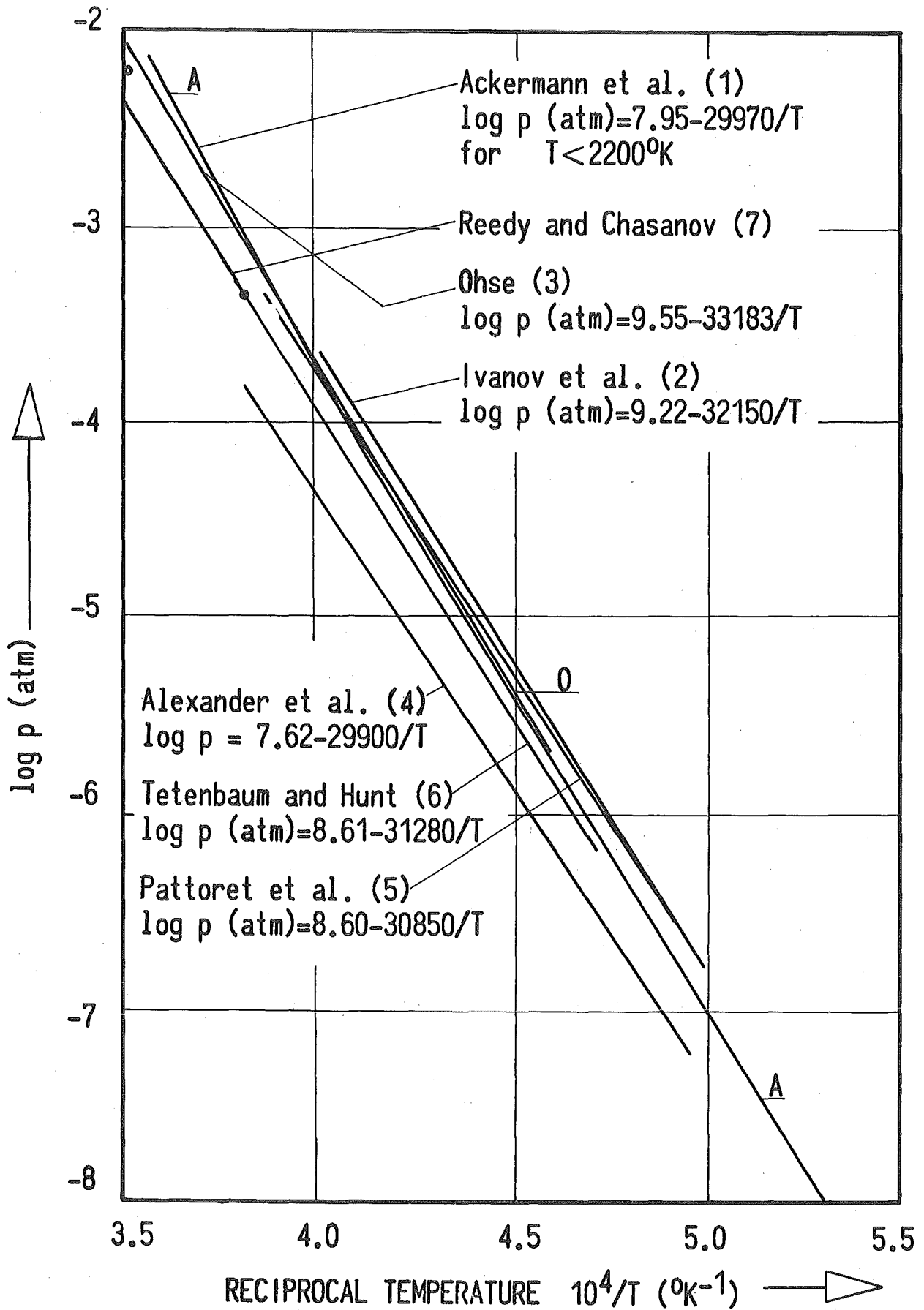
Fig.1. Partial pressures of uranium bearing species over UO$_2$
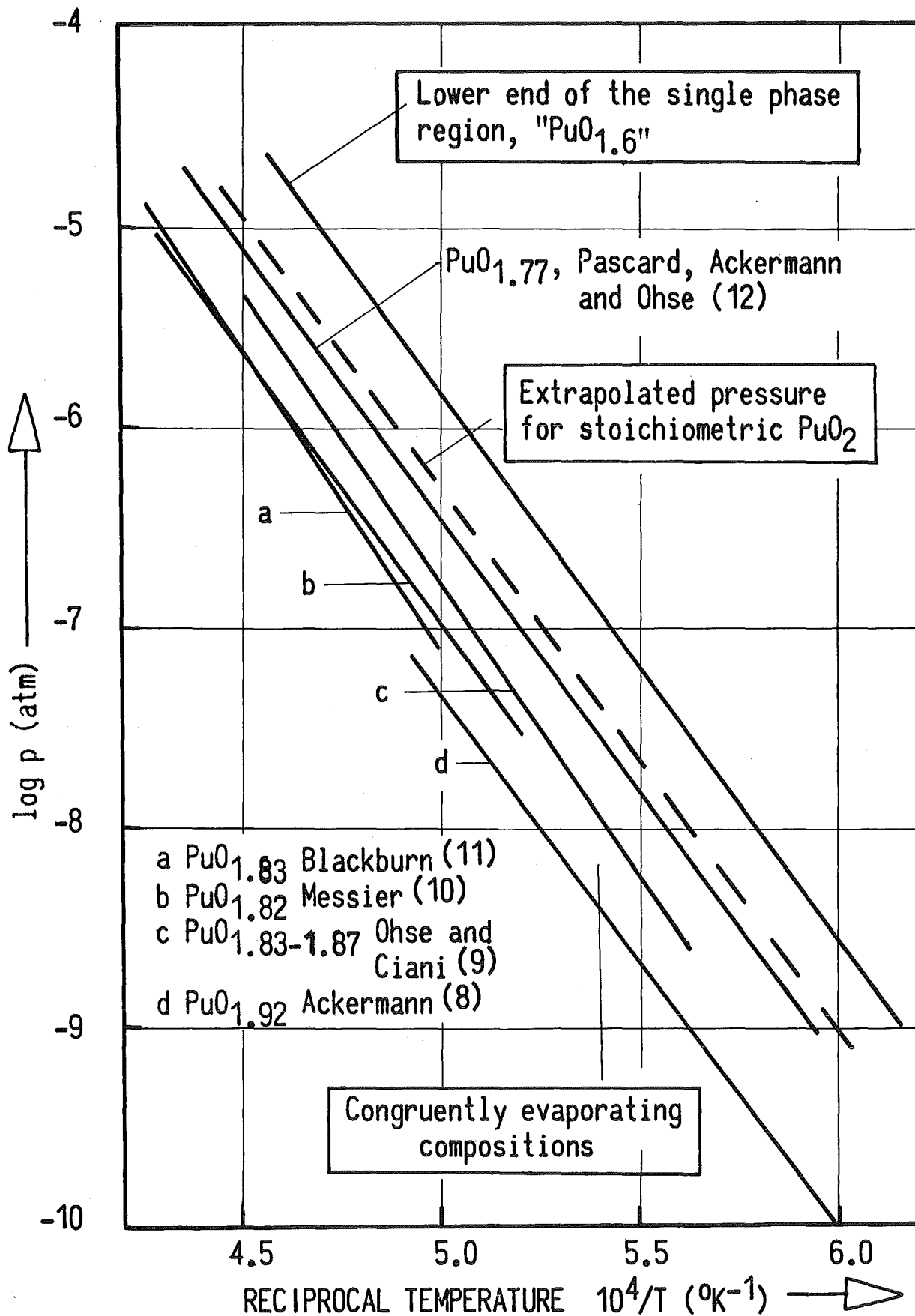
Fig.2: Partial pressures of the plutonium bearing species over PuO_{2-x}

$(U._{80} Pu._{20})O_{1.964}$

Battles et al (14)

$\log p_{UO_2}$ (atm)$=9.31-32352/T$

UO_2

UO_3

PuO_2

PuO

$(U._{85} Pu._{15})O_{1.97}$

Ohse + Olson (13)

$\log p_{UO_2}$ (atm)$=9.365-32436/T$

RECIPROCAL TEMPERATURE $10^4/T$ ($^{\circ}K^{-1}$) ⟶

Fig.3: Partial pressures of uranium and plutonium bearing
species over $(U,Pu)O_{2-X}$

quasi-congruently evaporating composition deviating only slightly from the compositions at which $(O/M)_s = (O/M)_g$ and $(U/Pu)_s = (U/PU)_g$, remained constant as shown by experiment because of the low rate of composition change throughout the time of effusion measurement. These compositions do not necessarily coincide with the minimum total pressure of the system. The quasi-congruently evaporating composition may be expected between the composition at the minimum total pressure and the composition at which $(O/M)_s = (O/M)_g$, because of the high oxygen potential in the mixed oxides and the mass dependent effusion rates. The quasi-equilibrium at which $(O/M)_s = (O/M)_g$ has been determined experimentally by Ohse and Olson /13/ for 15 mol. % PuO, at $(O/M)_s = 1.964$ while $(U/Pu)_s = (U/Pu)_g$ was found at $(O/M)_s = 1.968$. A rather flat vapour pressure minimum was obtained at $(O/M)_s = 1.97$. The UO_2 partial pressures measured by Battles et al /14/ over $(U_{0.80}Pu_{0.20})O_{1.964}$ as shown in Fig.3, are in almost complete agreement, with those of Ohse and Olson /13/, measured over $(U_{0.85}Pu_{0.15})O_{1.969}$ at practically the same plutonium valency of 3.6.
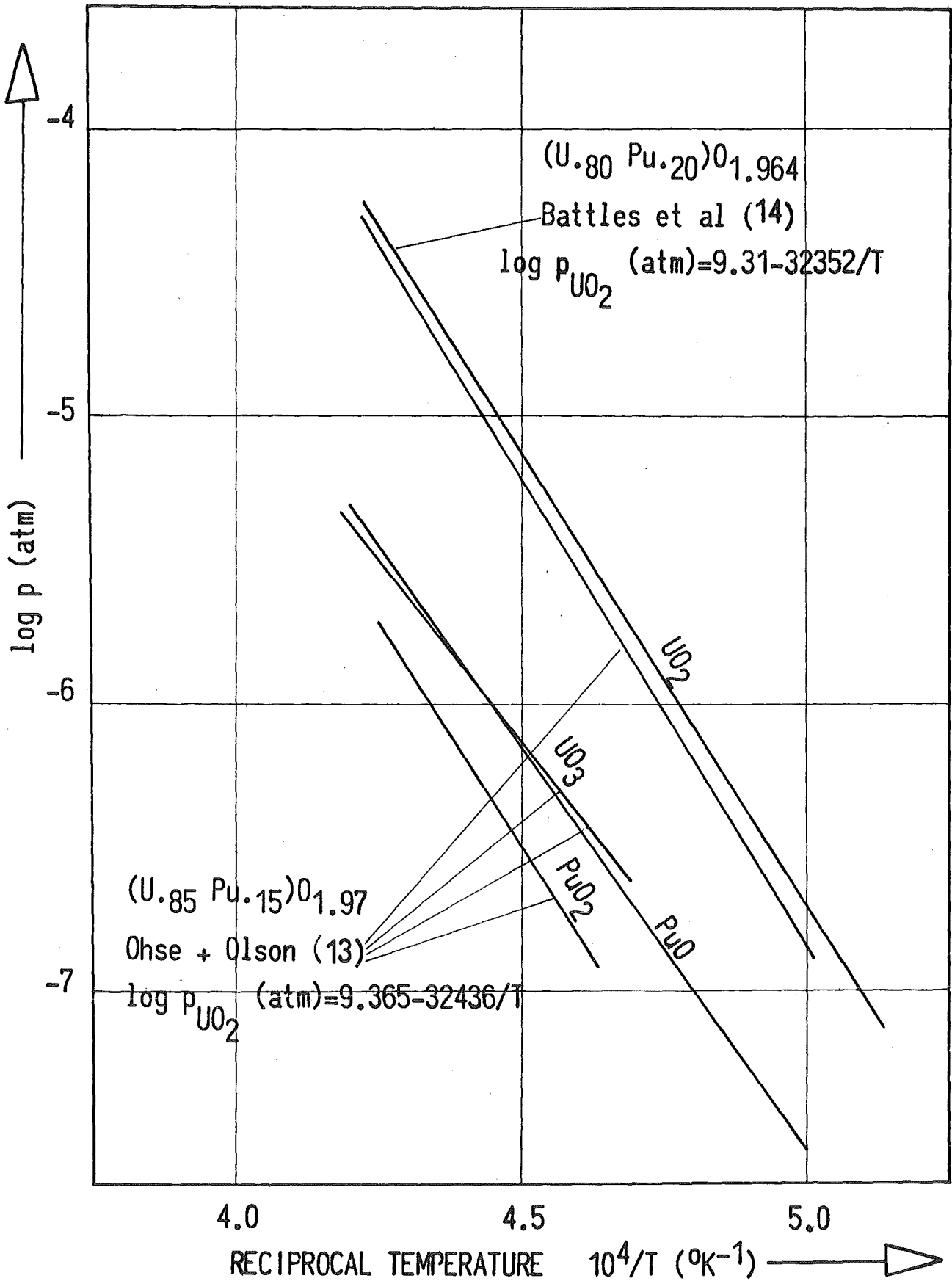
3. Theoretical extrapolation of data

The extrapolation of vapour pressure data to extreme temperatures may be performed directly on the measured low temperature data or by the use of suitable theoretical models. The result in both approaches is strongly dependent on the data selected.

The results of various measurements on UO_2 are presented in Fig.1. Though most of the pressure measurements, especially those obtained by the effusion technique, are in fairly good agreement, their slopes, representing the second law heat of sublimation ΔH_{sub}, vary by $\pm$ 10 kcal/mole. Linear extrapolations of the different log p vs. 1/T measurements to 5000°K, accounting for the heat of fusion, lead to an uncertainty in vapour pressure of the order of one magnitude.

Various theoretical approaches have been made to determine the critical data of pure UO_2. Meyer and Wolfe /16/ applied the principle of corresponding states and law of rectilinear diamter. Miller /17/ in a comparative review of the equation of state of UO_2, used the law of rectilinear diameters together with the pressure data of Ackermann et al /1/. Menzies /18/ fitted the data of Ackermann et al /1/ to the universal vapour pressure equation derived

from the principle of corresponding states. Robbins /19/ derived the limits of the equation of state by thermodynamic principles from the data of Ackermann et al /1/ and Ohse /3/. Booth /20/ estimated the critical data of UO_2 by the principle of corresponding states on behalf of the density measurements of Christensen /21/ and the pressure data of Ohse /3/. Gillan /22/ applied the theory of significant structures to UO_2 using the pressure measurements of Ohse /3/ and Tetenbaum /6/ arriving at a critical temperature of $6960^{\circ}K$ using the data of Ohse, and $9332^{\circ}K$ using the data of Tetenbaum. In the following report Fischer et al /23/ derived a new equation of state for UO_2 by the theory of significant structures, using the most recent data to predict the critical constants. The critical temperature of $7560^{\circ}K$ falls between the above values.

In a second step the influence of fission products on the equation of state of pure oxide fuels was included. Models have been presented by Brook /24/, Gabelnick and Chasanov /25/, Bogensberger et al /26/ and Ohse et al /27).

All these attempts are characterised by the application of models which were conceived for simple molecular liquids, and by the extrapolation of vapour pressure data over a range of several thousand degrees. These results can only be regarded as a guide, therefore the extension of the vapour pressure measurements for UO_2 and especially $(U,Pu)O_2$ as the fast breeder oxide fuel, up to $5000^{\circ}K$ are urgently required /27,28,29/.

4. Extension of measurement to 7000°K

4.1 Techniques of heat generation

At extreme temperatures classical vapour pressure techniques can no longer be applied since the high pressure build-up within the sample causes the breakdown of the molecular evaporation mode and entry into the "burst mode" or explosive errosion regime. In addition no crucible material exists which is able to withstand the extreme temperature.

A transition into the burst mode can only be avoided by restricting the heated volume to a thin surface layer. This however requires a pulsed heating technique with pulse times sufficiently short in order to keep the penetration depth of the heat wave at a minimum. The pulse width is determined on the one side by the necessity to reach the steady state and

guarantee sufficient accuracy in the measurement of the evaporated material and on the other side by the need to limit the penetration depth.

The power density must be high enough to obtain the required surface temperature, i.e. to balance the heat consumed by evaporation and losses by thermal conductivity and radiation. A linear extrapolation of the UO_2 pressure data to 5000 K leads to an expected evaporation rate of 1 m/sec. For microscopic evaluation a suitable depth of 100 µm leads to a pulse time of 100 µ sec. Assuming a target area of $1mm^2$ and a heat of sublimation of 150 kcal/mole a minimum power density of 10^7 W/cm^2 is required to evaporate 100 µm within 100 µs at 5000^oK. In order to obtain this high power density a well-focused beam is essential. This however can only be achieved by a laser beam, which does not undergo scattering to the same extent as an electron beam when entering a high density vapour jet.

Since the vapour pressure is given by the amount of evaporated material (depth), the surface temperature and pulse time, the power profile across the beam and the pulse profile as a function of time must be well defined. Only the Gaussian power profile, delivered by a single transversal mode, can fulfill the requirements given by the pyrometric temperature measurement discussed in section 4.4. Working in the microsecond time scale requires beam switching by electrooptical Pockels cells /30/ as used with solid state lasers. Therefore, a neodymium doped YAG laser, supplied by LASAG, was selected for surface heating.

4.2 Phenomena of läser surface heating

Solid Phase

Contrary to the isothermal Knudsen technique, surface heating is characterised by high temperature gradients within the surface layers, determined by optical absorption of the laser light, thermal conductivity and rate of evaporation. The quasi-steady state is finally established when the speed of the heat wave into the material and the speed of the evaporating front are equal. The penetration depth, i.e. the thickness of the heated layer, controls the temperature profile within the sample,

and by this the pyrometric temperature measurement, as shown in section
4.4. The position of the phase transition, governed by the temperature
profile, determines the thickness of the liquid layer.

Gas Phase

Molecules leaving the target surface have an initial velocity distri-
bution which is approximately Maxwellian /31/. This distribution gradually
changes with increasing distance from the surface as internal energy is
converted into forward motion. Within a certain layer thickness /32/
given by the number of collisions necessary to relax the internal energy,
thermal equilibrium with the surface can be assumed. Beyond this layer
the gas molecules accelerate to the local velocity of sound, and finally
to supersonic velocities /28,33,34/. The maximum value is limited by the ini-
tial enthalpy of the vapour. The expansion into vacuum is described gas
dynamically by a centered rarefaction wave /34,35/. The evaporating mole-
cules exert a recoil pressure on the evaporation surface determined by
the number of molecules and their momentum. This recoil pressure can
cause displacement of the liquid layer towards the edge of the crater,
in the case of sufficiently high penetration depth at lower temperatures.

Thermal ionisation increases with temperature causing optical ab-
sorption of the incoming laser light and of the radiation leaving the
surface. These phenomena are discussed in section 4.4.

4.3 Techniques for measuring pressure and temperature

Vapour pressure measurement

As in every dynamic technique the vapour pressure is determined by
measuring the rate of evaporation at a given temperature. This rate can
either be determined by an integral measurement such as target collection,
weight loss, evaporation depth and recoil momentum, or by a time resolved
technique such as mass spectrometric ion intensity measurement and, if
fast enough, recoil momentum or torsion technique.

In this work the direct determination of the depth was preferred
to recoil momentum /28.29/, since it eliminates integration over the

radial temperature profile. This is achieved by correlating the maximum depth of the hole, corresponding to the peak value of the Gaussian power profile, to the maximum temperature at this point.

Under conditions of rapid evaporation two effects, recondensation and a possible departure from equilibrium pressure, require special attention.

Free molecular evaporation is described by the equation:

$$\frac{1}{A}\left(\frac{dm}{dt}\right) = p_s \sqrt{\frac{M}{2\pi\ RT}}$$

where dm/Adt is the evaporation rate per unit area, p_s is the saturated vapour pressure, M is the mass of the evaporating molecules. At high rates of evaporation the increasing number of collisions in the vapour phase can lead to a backward flow of molecules and recondensation on the surface /34, 36/. Special attention has been paid therefore to any departure from linearity of the log p versus 1/T plot of the results with respect to this effect, or that of optical absorption, discussed in section 4.4.

Evaporation processes outside the congruently evaporating composition lead to depletion effects at the surface of the sample. Since solid state diffusion cannot restore the original surface composition fast enough, first experiments were conducted on sub-stoichiometric samples previously heated above their melting point, in order to approach the quasi-congruent compositions /13/. Therefore, possible deviations from equilibrium pressure by a change in the composition in the gas phase, taking place either by depletion or forced congruency, were reduced .

In a second phase the partial pressures of the different gaseous species will be determined by mass spectrometric measurement.

Temperature measurement

The main experimental difficulty is the accurate measurement of the true surface temperature. In principle there exist various methods for temperature determination.

The calculation of temperature from the measured laser energy by means of the heatbalance equation, given in section 4.4, cannot provide the required accuracy since the heat loss by reflection, thermal conductivity etc. are insufficiently known. In addition, it assumes a prior knowledge of the heat of evaporation, one of the paramters to be measured.

Indirect temperature determinations from the recoil momentum of the molecular beam assume complete knowledge of the ratio of all gaseous species (approximately nine in case of the ternary system U-Pu-O) as a function of temperature and composition (different heats of sublimation given by the slopes of log p versus 1/T curves). Moreover, the temperature profile across the target, given by the power density profile across the beam, needs to be known as accurately as its complicated time display. However, spatial and time resolution cannot be achieved by an integrating pendulum technique.

The calculation of temperature from the mass spectrometrically determined intensity ratio of two evaporating species assumes the knowledge of thermodynamic data on heat of evaporation over the liquid range.

In addition to the various techniques mentioned above, gas temperature measurements will become of importance in the region where ionisation and absorption in the gas phase inhibits surface temperature measurement. This will be of increasing significance above 5000° to 6000°K. Here emission or absorption spectroscopy may become important tools to proceed to higher temperatures. However, the measurement of the relative intensities of the spectral lines emitted by the vapour requires the spectroscopic data of UO_2 at temperatures where it is only partly known /29/.

4.4. Optical Pyrometry

Optical pyrometry allows the measurement at the small, central surface area where the temperature is almost constant. The central temperature correlating to the maximum depth of the hole, can be directly calculated from the average temperature of this measured area.

In addition to spatial resolution, time resolution can be obtained by the display of the fast photomultiplier signal on a wide bandwidth storage oscilloscope. This enables rise time of temperature versus power

density of laser beam to be investigated, and finally permits correlation of the time display of surface temperature to the amount of laser evaporated material.

The main problems are:
- the extrapolation of emissivity data,
- the influence of the temperature profile inside the sample on the total measured intensity
- the optical absorption of radiation in the gas jet above the surface.

Emissivity

The most reliable emissivity data /37/ were extrapolated after a critical review of all available literature data /38/. According to measurements of McMahon and Wilder /39/ on the spectral emissivity of rare earth oxides and zirconium oxide, no change was observed when passing through the melting point. This can be checked by vapour pressure measurements above and below the melting point, which should indicate any marked change in emissivity.

A multi-wavelength pyrometer has been constructed to eliminate the remaining uncertainties in spectral emissivity, by measuring the relative emissivity versus wavelength. For the final measurement, wavelengths of equal emissivity are selected, such that, according to Planck's spectral distribution law, sufficient sensitivity is obtained.

Influence of Temperature Profile

In order to ensure that there is no major error in the temperature measurement due to the temperature profile in the sample, the difference in intensity between a uniformly heated sample and one with the temperature profile calculated by the model of Dabby and Paek /40/ was determined at $5000^{\circ}K$.

Dabby and Peak set up the heat balance equations, assuming a constant absorption coefficient for the laser light, heat conduction inside the sample, and vaporization at the surface, leading to a moving boundary. The steady state is characterized by a constant rate of vaporization. If the coordinate z is referenced to the moving surface, the steady state temperature distribution is:

$$T(z) = T_v \left[e^{-\beta z} - \frac{\gamma}{\alpha - \beta} (e^{-\alpha z} - e^{-\beta z}) \right]$$

where

$$\beta = \frac{\rho \, \dot{Z} \, C_p}{K} \, , \qquad \gamma = \frac{I}{K \, T_v} \, ,$$

and the notation is the following:

T_v = 5000° K surface temperature

C_p = 0.42 J/g. K specific heat

L_v = 1830 J/g heat of sublimation

K = 0.033 W/g K cm thermal conductivity

ρ = 10.4 g/cm^3 density

$\dot{Z}$ = 130 cm/sec speed at which the surface recedes

α cm^{-1} = optical absorption coefficient

I,W/cm^2 = laser intensity

In the steady state, I may be expressed as

$$I = (L_v + C_p \, T_v) \, \rho \, \dot{Z}$$

The values of the thermal constants are reasonable estimates for 5000°K and $\dot{Z}$ is an experimental value, extrapolated to 5000°K. The absorption coefficient α is more difficult to estimate. Following the arguments given by Wooten /41/, the equation

$$\alpha = \frac{4 \, \pi \, \sigma}{n \, c}$$

can be used, even in the case of strong absorption. Literature values /42/ for the index of refractivity, n of UO_2 vary between 2.29 and 2.58. The

wave length is in the range 4500 $\overset{o}{A}$ to 8000 $\overset{o}{A}$. The following equation for the electrical conductivity σ ($\Omega^{-1}cm^{-1}$), above $1900^{\circ}K$ was proposed by Alper /43/

$$\sigma = 2.10 \times 10^{-2} \; T^{1.4} \; \exp \; (-0.916 \; eV/kT)$$

If this empirical fit is used in the above equation, α at 5000 K can only be determined with a rather large uncertainty. The fit for σ does not take into account the dependence on the frequency. For optical frequencies, the conductivity increases substantially due to electron transitions. It is believed therefore that the resulting value, α = $6 \times 10^4 cm^{-1}$ at $5000^{\circ}K$ represents a lower limit, in spite of additional uncertainties due to the extrapolation in temperature, and the neglect of the dependence on stoichiometry. In view of the uncertainties which are involved anyway in extrapolating all the necessary data to $5000^{\circ}K$, phase changes were neglected in this analysis.

The radiation intensity at the surface I_s can be calculated from Planck's law, and the radiative transfer equation. One obtains in good approximation

$$I_s \; (T) = C_1 \int_0^\infty \alpha \; dx \; \frac{e^{-\alpha X}}{\exp \; (\frac{h\nu}{kT(x)}) - 1}$$

The relative difference in intensity, calculated for the temperature distribution of Fig.1 and for constant temperature T_v, is $\Delta I/I_s$. It can be converted to an error in temperature, $\Delta T/T_v$, from the relation

$$\frac{\Delta T}{T_v} = \frac{\Delta I}{I_s} \frac{kT}{h\nu}$$

The results, for a few reasonable values of α, including the lower limit are shown in Table 1.

The radiation intensity at the surface depends on the temperature profile, as shown in Fig.4. A broad peak leads to an overestimation of the temperature, while for narrow peaks, the temperature is underestimated. According to the above results, the error in the temperature measurement due to the effect of the temperature profile is indeed negligibly small at $5000^{\circ}K$.
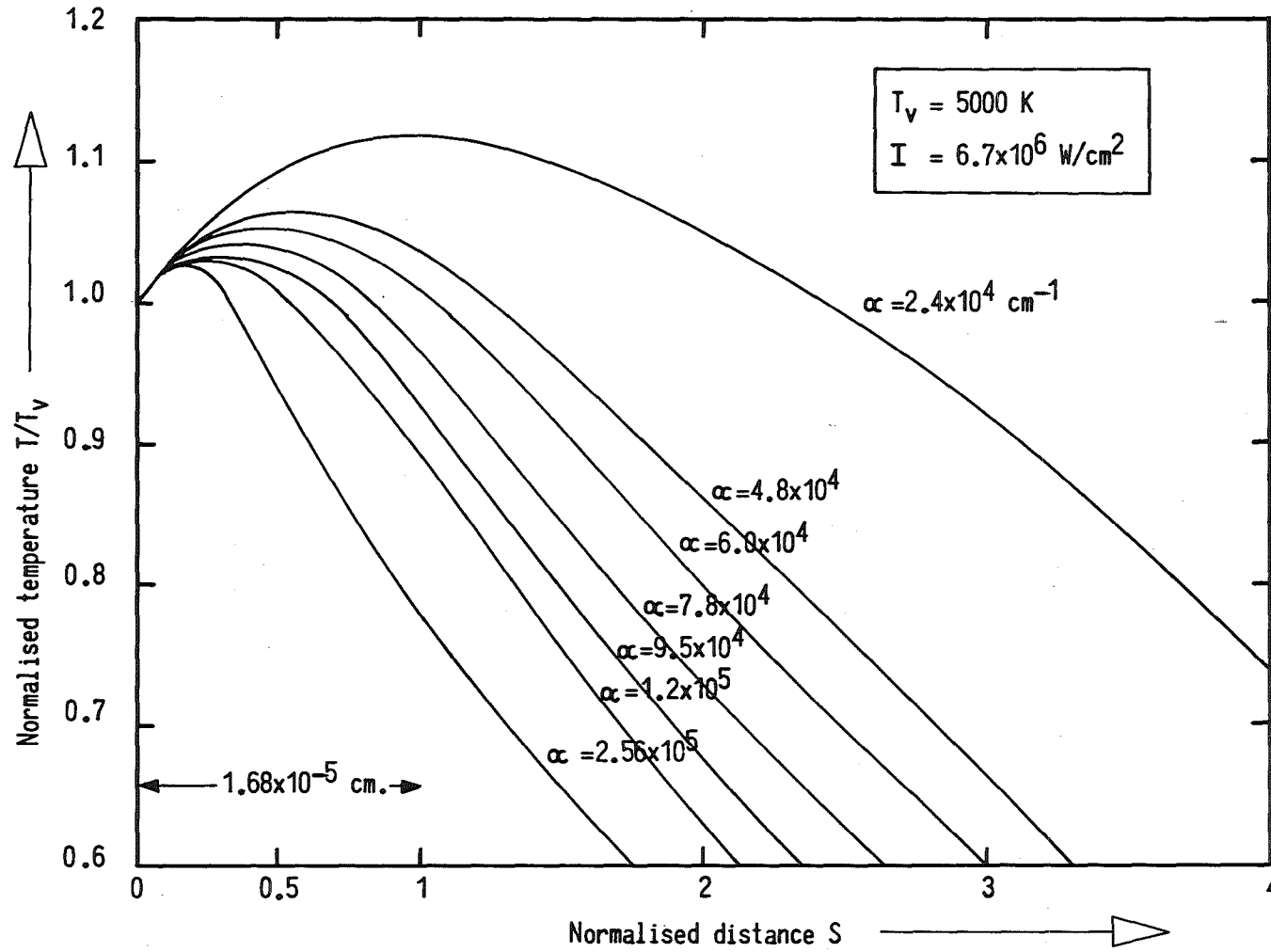
Fig. 4. Temperature profile in the sample for different absorption coefficients.

Optical_absorption

Optical absorption depends on the degree of ionization of the gas phase which increases with temperature.

Since the gas phase over $(U,Pu)O_2$ consists mainly of UO_2 molecules, the absorption properties of UO_2 at extreme temperatures have been considered. The degree of thermal ionization in the high density gas cloud above the surface has been estimated by use of the Saha equation, to be less than 1 % at 5000°K. Neglecting resonance absorption processes, standard Bremsstrahlung absorption theory /35/ leads to a total absorption coefficient of 1.564 cm^{-1} for 0.65 µm, used for the optical pyrometric measurements, and 1.224 cm^{-1} for the 1.06 µm wavelength of the Nd: YAG laser. Assuming a pressure of 100 atm at a surface temperature of 5000 K, corresponding to a gas density of 1.47×10^{20} molecules/cm^3, and an absorbing layer of 0.5 mm /36/, the absorption of 1.06 µm laser light is approximately 6 %, and that of the 0.65 µm pyrometer wavelength is of the order of 7 %, leading to an error of approximately 1.5 % in temperature measurement. The absorption figures suggest that at temperatures in excess of 5000°K the gas temperature could be evaluated above that of the solid. Below 5000°K absorption effects are sufficiently small to be neglected.

Optical pyrometry, because of the spatial and time resolution, will therefore, within the limitations given by optical absorption, provide the best means for measuring temperature and analysing the laser evaporation phenomena.

4.5 Experimental lay-out

Fig.5 shows the experimental arrangement for vapour pressure studies up to extreme temperatures of 7000°K.

The uranium-plutonium oxide pellets were carefully melted at 2800°C in order to obtain samples of as nearly 100 % theoretical density as possible, with a minimum of pores or bubbles. To avoid minor cracks, the samples were slowly cooled to room temperature at rates of 200°K/h. This is important since, if the laser beam impinges on bubbles or cracks, the resulting explosion like reaction disturbs the measurements. In addition, the samples were polished to below a roughness of 0.1 µm in order to allow an accurate microscopic evaluation of the depth. The pellets were finally outgassed in the electron beam furnace and mounted on an X-Y table before being used as the laser target.

Optical Pyrometer

High-Temp. Furnace

Mass Spectrometer

Power Supply
Thermostat

Iris aperture
Shutter
Interference Filter

Fast Photo-Multiplier

Micro-Objective

Micro-Aperture

BW

L   P

FW
PG

Glove Box

Quadrupole

P   FW   BW

PG

W-cell

X
Y

Diff. Amplifier

Digital Volt-Meter

Reference Voltage

Amplifier

RF / DC Generator

Power Supply

1   2   3   4   5   6   7   8   9

Nd: YAG LASER

18   17   16   15   14   13   12   11   10   9

MULTI - CHANNEL
STORAGE OSCILLOSCOPE

1.Temperature Signal
2.Mass spectrometric
   ion intensity signal
3.LASER energy signal
4.LASER pulse profile

Trigger Circuit

Power Supply

High-Vacuum Pumping Device

Power Supply Electron Beam Furnace

1: He-Ne-LASER
2: Mirror
3: Polarizer

4: Oscillator
5: Mode Selector
6: Mirror

7: Photodiode
8: Beam Switch
9: Beam Reflector

10:   I Amplifier
11: II Amplifier
12: III Amplifier

13: Pockels-cell
14: Analyzer
15: Photodiode

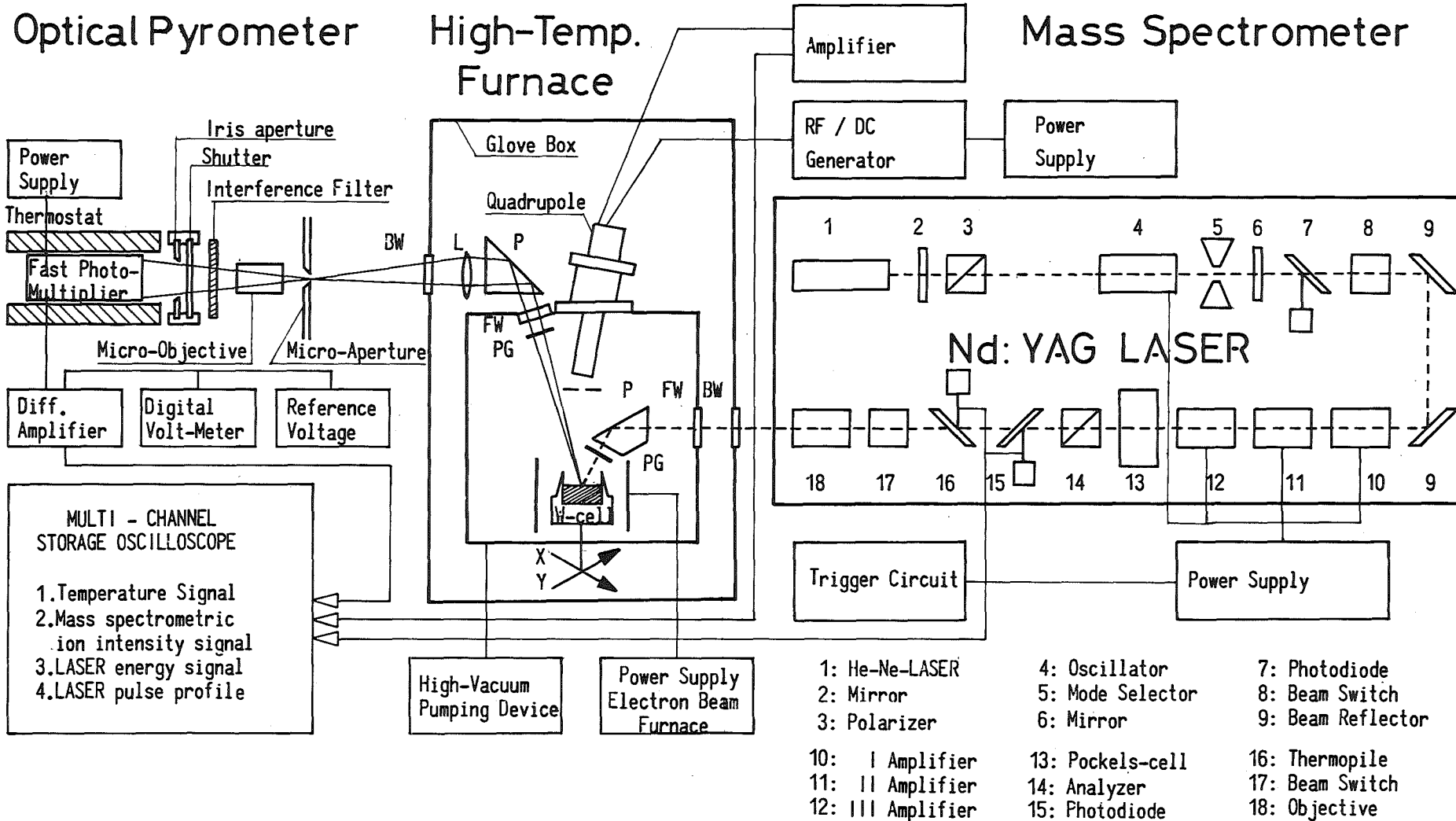16: Thermopile
17: Beam Switch
18: Objective

-16-

Fig. 5 : Schematic display of vapour pressure studies up to 7000°K by LASER surface heating, fast temperature recording and mass spectrometric ion intensity measurement.

A neodymium-doped YAG laser supplied by LASAG, with three amplifier units, delivering a single transversal mode in a Gaussian power profile in the pulse range from 1 µs to 5 ms, with a maximum power density of the order of 10^7 W/mm^2, was chosen for surface heating.

Fig.6 shows the complete laser pulse and complete stabilisation of the relaxation oscillations before further amplification.

Fig.7 presents the final laser pulse after being chopped by the Pockels cell. During each laser shot the temperature signal, ion intensity and laser energy were recorded on a fast storage oscilloscope. The temperature was measured by a fast photomultiplier, calibrated on the International Practical Temperature Scale (IPTS) /44/.

Finally Fig.8 gives the temperature signal measured on the target surface as a function of time during laser pulse heating. As shown here, the display of the temperature signal is clearly defined by the laser pulse, allowing the analysis of the influence of power density on its rise time as a function of laser light absorption and rate of change in optical absorption coefficient.

Since the rise time in surface temperature is a function of the power density of the laser beam, an exact knowledge of the surface temperature curve during the pulse is indispensable for accurate vapour pressure measurements. In complete analogy to the rise time, the maximum surface temperature during the pulse depends mainly on the power density profile across the focus of the laser beam. The total temperature range up to 7000°K can be achieved, using the same laser energy, simply by strongly increasing the power density by proportionally reducing pulse times.

Since the vapour pressure is evaluated from the amount of material evaporated during a given time of surface heating, the maximum depth has to be related to the central temperature. The pyrometric measurement requires a finite surface and deviations from the central temperature have to be accounted for in the evaluation. In order to avoid strong deviations, the measured area was kept as small as possible. The optical measurement of the target was restricted therefore to a surface of 160 µm in diameter, by choosing a suitable arrangement of diaphragm and lenses. According to the size of the focal spot and the Gaussian power profile in the focus of the laser beam, the power decrease across this target corresponds to less than 2.3 % of the peak power.
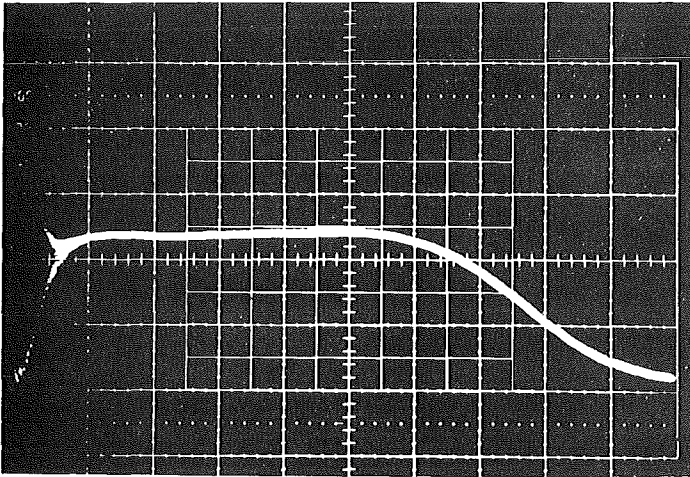
Fig.6 Complete laser pulse
      showing stabilisation
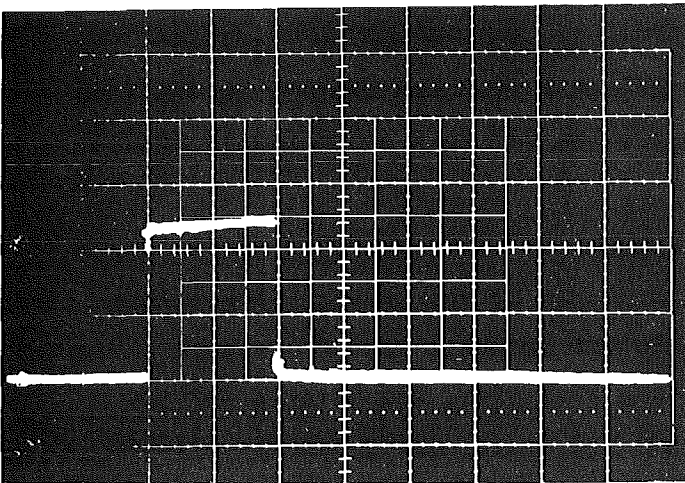   of relaxation oscillations.

Fig.7 Final laser pulse after
      chopping by Pockels cell.
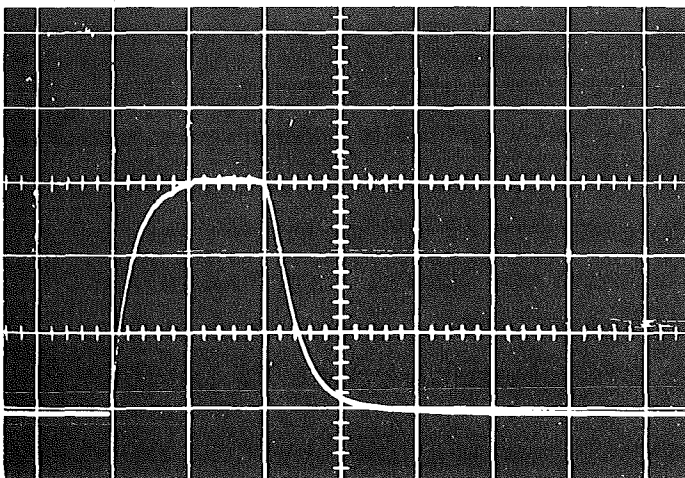

Fig.8 Temperature signal of
      the target during laser
      heating (during experiments
      the base line is offset
      to increase resolution).

The calculation of the required central temperature from the temperature signal of this target area, already corrected for emissivity and transmissivity of all interposed windows and prism, includes the power density profile, photomultiplier calibration and extension of the temperature scale and finally the diffraction effect given by the different conditions of calibration without gradient and measurement under a temperature gradient. The maximum depth of the hole is measured microscopically by making use of special optics of extremely small focal depth, allowing measurements down to the order of 1 μm.

The gas phase above the ternary oxides consists, as was shown in previous studies /13/ of a large number of gaseous species, namely PuO_2, PuO, Pu, UO_3, UO_2, UO, U, O_2 and O. The data for their thermal dissociation energies, and appearance and fragmentation potentials are still the subject of considerable uncertainties. The partial pressures and heats of sublimation, i.e. the slopes of appropriate log p versus 1/T curves, do not only differ from one gaseous species to another, which means that their ratio is a function of temperature, but depend strongly on composition changes of the solid (Pu/(U+Pu),O/M). Therefore, mass spectrometric ion intensity measurements are required to check the molecular evaporation mode, and to obtain the required partial pressures and partial heats of sublimation in order to allow an extrapolation towards higher temperatures, and enable a study of the evaporation processes to be made.

5. Results and Discussion

5.1 U-Pu-O

In view of its application as a fast breeder oxide fuel, the composition chosen for vapour pressure studies was 20 mol % PuO_2 at a stoichiometry of O/M = 1.96. The pressure data are presented in Fig.9 in a log p versus 1/T diagram. Apart from pressure measurements, molecular evaporation was checked by ion intensity measurements, using an E.A.I. mass spectrometer.

Partial pressures over solid uranium plutonium oxides were measured by both Ohse and Olson /13/, and Battles et al /14/. The partial pressure of UO_2 from both sets of measurements is in good agreement.

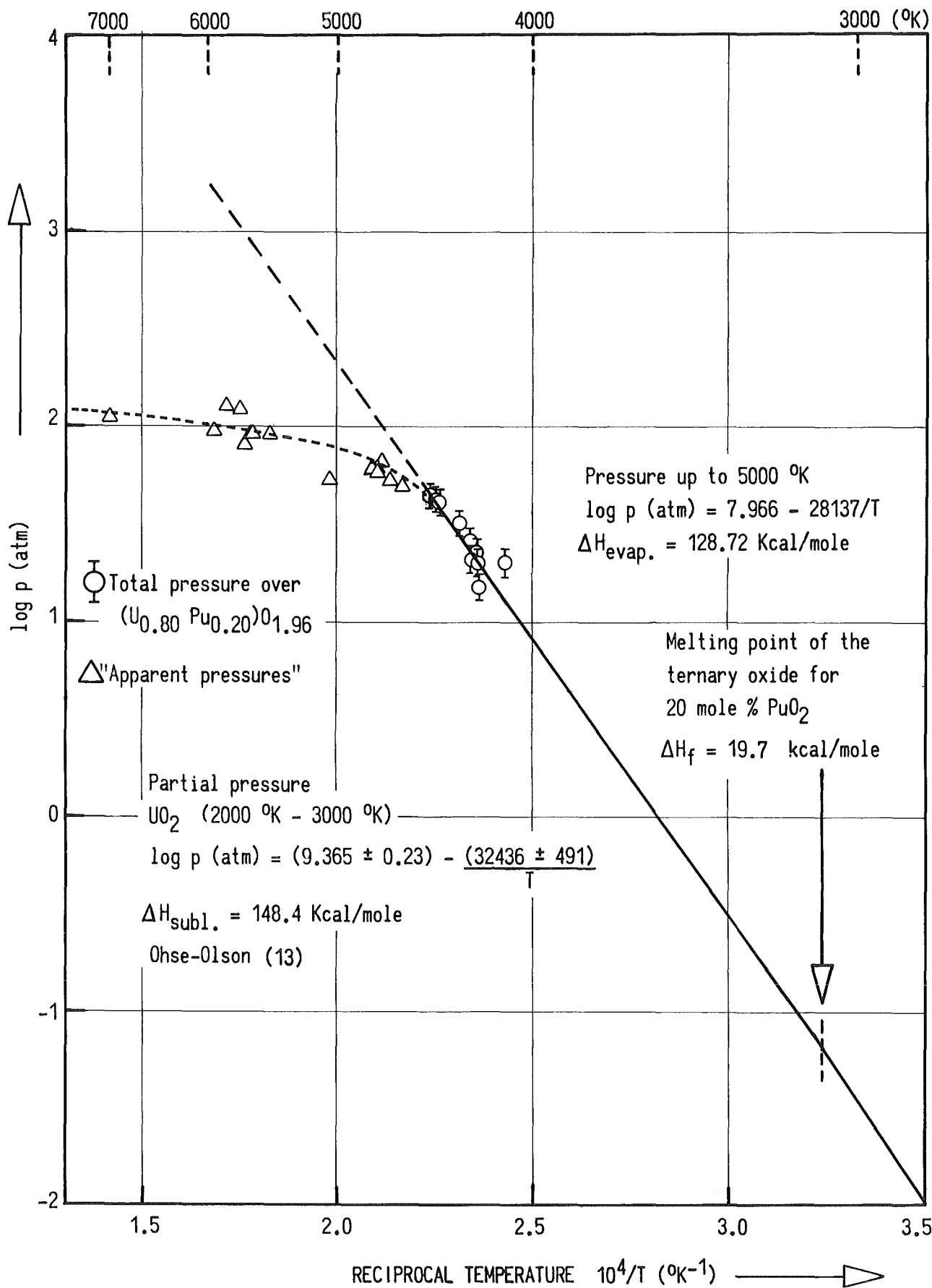Fig.9. Extended vapour pressure measurement up to 7000 °K over $(U_{0.80} Pu_{0.20})O_{1.96}$ compared to previous data over the solid.

The data of Ohse and Olson /13/

$$\log p_{UO_2}(atm) = (9.365 \pm 0.23) - \frac{(32436 \pm 491)}{T}$$

with a heat of sublimation of ΔH_{sub} = 148.4 kcal/mol, corresponding to the same plutonium valency as in the present experiments, were extrapolated to the melting point of $(U_{0.80}Pu_{0.20})O_{1.96}$, accepted to be 3073°K.

A least-squares fit through the measured data above 4000°K and the vapour pressure at the melting point, obtained from the previous experimental measurement /13/ over the solid phase, yields the equation:

$$\log p \ (atm) = 7.966 - \frac{28137}{T}$$

with a heat of evaporation of ΔH_{evap} = 128.7 kcal/mol.

The heat of fusion calculated from the difference in slopes of the vapour pressure measurements over the two temperature ranges below and above the melting point is ΔH = 19.7 kcal/mol. This value is in excellent agreement with the differential thermal analysis (DTA) value obtained by Ohse, Kerr and Schmit /45/ for 20 mol % PuO_2 and a composition of O/M = 1.96, ΔH_f = 20 kcal/mol, and that of Ogard, Reavis and Leary /46/, ΔH_f = 19.4 kcal/mol.

5.2 U-O

In order to check the various attempts to extrapolate the UO_2 vapour pressure data towards the critical temperature, a series of pressure measurements was made at 5000°K. The technique used was the same as that adopted for the mixed oxides, in which the pellet was first melted and then polished to a roughness below 0.1 μm. The results are given in Table 2. The data analysis was performed as for the U-Pu-O system. The literature data of Ackermann et al /1/, Ohse /3/, Alexander et al /4/, Tetenbaum et al /6/, Pattoret et al /5/, Ivanov et al /2/ and Reedy and Chasanov /7/ for the solid UO_2 were extrapolated to the melting point of UO_2 at 3133 K using an averaged equation of:

$$\log p \ (atm) = 8.846 - \frac{31506}{T}$$

with ΔH_{sub} = 144.1 kcal/mol. A least-squares fit through the average vapour pressure at the melting point and the measured data above 4000 K yields the equation:

$$\log p \text{ (atm)} = 7.7 - \frac{27900}{T}$$

The heat of evaporation amounts to 127.6 kcal/mol, which, compared with the average heat of sublimation over the solid phase of ΔH_{sub} = 144.1 kcal/mol yields a heat of fusion of ΔH_f = 16.5 kcal/mol, only slightly below the value of Leibowitz et al. /47/ of 17.7. kcal/mol.

5.3 Discussion

As shown above, the first vapour pressure data measured over the liquid phase of both $(U,Pu)O_2$ and UO_2 are in reasonable agreement with the data over the solid phase and the calorimetrically measured heat of fusion. The comparison of the heat of evaporation and sublimation presents a most critical and sensitive method for testing these experimental data. One must be aware however of the possibility that the heat of evaporation may not be constant, but decreases towards the critical temperature, estimated to be 7560 K /23/. This would lead to a slightly higher heat of evaporation immediately above the melting point than the averaged value of ΔH_{evap} = 127.6 kcal/mol in the case of UO_2. Consistency between the heats of evaporation and sublimation, and the heat of fusion could then only be obtained by a slightly higher heat of sublimation, given by excluding the transpiration measurements as proposed in the following "critical assessment of the equation of state data for UO_2" /23/. Good agreement would then be obtained with the previous effusion measurements over solid UO_2 /3/.

The observed deviation of the "apparent pressure data" around 5000°K appears as the first measurements show, to depend strongly on the length of the heating laser pulse. The departure to lower pressures can be explained by either a temperature measurement higher than the actual surface temperature, or by recondensation effects. Gas temperatures higher than surface temperatures can only be realised by absorption of laser light in the gas phase, whereas recondensation results from high pressures above the target surface.

The optical absorption of laser light depends mainly on the density and degree of ionisation of the gas jet leaving the surface. The figures calculated in section 4.4 suggest that the gas temperature at 7000°K could well be elevated above that of the solid. At 4500°K the temperature error introduced by absorption can be neglected.

Present estimates of critical temperature give values ranging from 5000° to $10,000^\circ$ K, depending on the choice of the input data. First test measurements up to 7000°K, i.e. well into this range, were found to fit smoothly onto the dotted line shown in Fig.9 when using a constant time of laser pulse heating. The "apparent pressure data" might in addition indicate a high dynamic pressure above the solid, preventing free evaporation. This effect is empirically well known in laser machining, where best results were obtained using a "spiking" or modulated beam /49,50/.

The third possibility, introducing errors in vapour pressure measurements, is given by fast or non-accounted changes in molecular weight of the vaporizing species and surface composition, in this case by the contribution of oxygen and surface depletion effects. This was eliminated by choosing the quasi-congruently evaporating composition. At this composition the contribution from O atoms and O_2 molecules can be neglected.

REFERENCES

/1/ R.J. Ackermann, P.W. Gilles and R.J. Thorn, J.Chem.Phys. 25 (1956) 1089

/2/ V.E. Ivanov, A.A. Krughlykh, V.S. Pavlov, G.P. Kovtan and V.M. Amonenko, Thermodynamics of Nuclear Materials (Proc. Symp. Vienna 1962), IAEA, Vienna (1962) 735 (in Russian)

/3/ R.W. Ohse, J.Chem. Phys. 44 (1966) 1375

/4/ C.A. Alexander, J.S. Ogden and G.W. Cunningham, Batelle Memorial Institute Rep. BMI-1789 (1967)

/5/ A. Patteret, I. Drowart and S. Smoes, Thermodynamics of Nuclear Materials 1967 (Proc. Symp. Vienna,1967) IAEA, Vienna (1968) 613

/6/ M. Tetenbaum and P.D. Hunt, J.Nucl.Mater. 34 (1970) 86

/7/ G.T. Reedy and M.G. Chasanov, J.Nucl.Mater. 42 (1972) 341

/8/ R.J. Ackermann, R.L. Faircloth and M.H. Rand, J.Phys.Chem. 70 (1966) 3698

/9/ R.W. Ohse and V. Ciani, Thermodynamics of Nuclear Materials 1967 (Proc. Symp. Vienna, 1967) IAEA, Vienna (1968) 545

/10/ D.R. Messier, J.Am.Soc. 51 (1968) 70

/11/ P.E. Blackburn, A.D. Tevebaugh, and J.D. Bingle, USAEC Rep. ANL-7575 (1968)

/12/ International Atomic Energy Agency refers to data provided by R.J. Ackermann, C.E. Holley Inr, R.N.R. Mulford, R.W. Ohse and R. Pascard, The Plutonium Oxygen and Uranium-Plutonium Oxygen Systems: A Thermochemical Assessment, Technical Report Series No. 79, IAEA, Vienna (1967) 41-59, see also 85-86

/13/ R.W. Ohse and W.M. Olson, Plutonium 1970 and Other Actinides (Proc. 4th Int. Conf. Santa Fe, New.Mex. 1970, W.N. Miner, Ed.) Vol.2 AIMMPE, New York (1970) 743

/14/ J.E. Battles, W.A. Shinn, P.E. Blackburn and R.K. Edwards, Plutonium and other Actinides (Proc. 4th Int. Conf. Santa Fe, New Mex. 1970, W.N. Miner, Ed.) Vol.2, AIMMPE, New York (1970) 733

/15/ R.J. Ackermann and R.J. Thorn, Thermodynamics (Proc. Symp. Vienna, 1965) Vol.1, IAEA, Vienna (1966) 243

/16/ R.A. Meyer and B.E. Wolfe, Trans.Am.Nucl.Soc. 7 1 (1964) 111

/17/ D. Miller, USAEC Rep. ANL-7120 (1965) 641

/18/ C. Menzies, UKAEA Rep. TRG-1159 (D) (1966)

/19/ E.J. Robbins, UKAEA Rep. TRG-1344 (D) (1966)

/20/ D.L. Booth, UKAEA Rep, TRG-1759 (R/X) (1968, 1974)

/21/ J.A. Christensen, J.Amer.Ceram.Soc., 46 (1963) 607

/22/ M.J. Gillan, Thermodynamics of Nuclear Materials 1974 (Proc. Symp. Vienna, 1974), IAEA, Vienna (1975), Paper IAEA-SM-190/16

/23/ E.A. Fischer, P.R. Kinsman and R.W. Ohse, following report

/24/ A.J. Brook, UKAEA Rep. SRD-13 (R) (1972)

/25/ S.D. Gabelnick and M.G. Chasanov, USAEC Rep. ANL-7867 (1972)

/26/ H.G. Bogensberger, E.A. Fischer and P. Schmuck, Report presented to Am.Nucl.Soc.Conf. on Fast Reactor Safety, Beverley Hills, April 1974

/27/ R.W. Ohse, P.G. Berrie, H.G. Bogensberger and E.A. Fischer, Thermodynamics of Nuclear Materials 1974 (Proc. Symp. Vienna, 1974), Vol.1 IAEA, Vienna (1975) 307

/28/ M. Bober, H.-U. Karow and K. Schretzmann, Thermodynamics of Nuclear Materials 1974 (Proc. Symp. Vienna 1974), IAEA, Vienna (1975) Paper IAEA-SM-190/34

/29/ N. Asami, M. Nishikawa and M. Taguchi, Thermodynamics of Nuclear Materials 1974 (Proc. Symp. Vienna, 1974) IAEA, Vienna (1975), Paper IAEA-SM-190/3

/30/ Laser Handbook, Vol.1 (Eds. F.T. Arecchi and E.O. Schulz-Dubois) North-Holland, Amsterdam (1972)

/31/ P.S.P. Wei, D.J. Nelson and R.B. Hall, J.Chem.Phys. 62 (1975) 3050

/32/ V.A. Batanov, F.V. Bunkin, A.M. Prokhorov and V.B. Federov, Sov. Phys. JETP 36 (1973) 654

/33/ O.N. Krokhin, Laser Handbook, Vol.2 (Eds. F.T. Arecchi and E.O. Schulz-Dubois) North-Holland, Amsterdam, (1972) 1371

/34/ S.I. Anisimov, Sov.Phys.JETP 27 (1968) 182

/35/ Ya.B. Zel'dovich and Yu.P. Raizer, Physics of   Waves and High-Temperature Hydrodynamic Phenomena, Vol.1 (Eds. W.D. Hayes and R.F. Probstein) Academic Press, New York and London (1966)

/36/ V.A. Batanov, F.V. Bunkin, A.M. Prokhorov and V.B. Federov, Sov. Phys. JETP 36 (1973) 311

/37/ F. Cabannes, Private Communication to the Authors

/38/ G. Neuer, R. Brandt and G. Haufler, A Literature Study of the Thermal Conductivity and Emission Rate of Solid UO_2, IRS Rep. SB3 (1973), in German

/39/ W.R. McMahon and D.R. Wilder, J.Am.Ceram.Soc.51 (1968) 187

/40/ F.W. Dabby and U.C. Paek, IEEE J. Quantum Electronics QE8 (1972) 106

/41/ F. Wooten, Optical Properties of Solids, Acadm. Press, New York and London (1972)

/42/ J. Belle, Uranium Dioxide Properties and Nuclear Application USAEC (1962)

/43/ A.M. Alper, High Temperature Oxides, Part II, Academ. Press New York and London (1970)

/44/ IUPAC, Division of Inorganic Chemistry, Commission of High Temperatures and Refractories, Cooperative Determination of the Melting Point of Alumina, (Ed. S.J. Schneider) Pure and Applied Chem. 21 (1970) 117

/45/ R.W. Ohse, S.A. Kerr and M. Schmit, in preparation

/46/ A.E. Ogard, J.G. Reavis and J.A. Leary, Proc. 16th Conf. in Remote Systems Technology, USA (1969) 295

/47/ L. Leibowitz, M.G. Chasanov, L.W. Mishler and D.F. Fischer, J.Nucl.Mater. 39 (1971) 115

/48/ R.W. Ohse, P.G. Berrie, G.D. Brumme and P.R. Kinsman, Proceedings of the 5th International Conference on Plutonium and other Actinides, September 1975, Baden-Baden, North-Holland Publishing Company

/49/ E. Kocher, L. Tschudi, J. Steffen and G. Herziger, IEEE J.Quantum Electronics QE8 (1972) 120

/50/ G. Herziger, R. Stemme and H. Weber, IEEE J. Quantum Electronics QE10 (1974) 175

Part II: Critical Assessment of Equation of
State Data for UO_2

E.A. Fischer

Institut für Neutronenphysik und Reaktortechnik

P.R. Kinsman, R.W. Ohse

Europäisches Institut für Transurane

1. Introduction

Reliable equation of state data for UO_2 fuel, up to temperatures of 5000°K, are required with high priority for the analysis of hypothetical fast reactor accidents. In the years 1963 to 1968, several authors derived such data up to the critical point, from the principle of corresponding states /1,2,3,4/. The principle, which was derived from statistical thermodynamics under certain simplifying assumptions, states that a universal (P-V-T) relationship, in reduced variables, holds for all " simple" materials. It was shown by Miller /2/ that the equation of state derived for UO_2 depends strongly on the input data, usually experimental vapour pressure measurements. Menzies /3/ used an averaged vapour pressure equation for the extrapolation, and his equation of state was used in several laboratories for reactor accident analysis. Gillan /5/ has applied the significant structure theory to UO_2, and calculated two sets of critical data using the vapour pressure data of Tetenbaum and Hunt /6/ and Ohse /7/, predicting critical temperatures of 9330°and 6960°K, respectively.

Since Menzies' evaluation additional thermodynamic measurements have been made. Thus experimental data on solid phase enthalpy is available to the melting point /8,9,10/ together with vapour pressure data /11,7,6/. For liquid UO_2 there are data on enthalpy /12/, density /13/, and compressibility /14/, but confined to a small range of temperature just above the melting point. Recently experimental techniques for vapour pressure measurement have been developed, whereby temperatures of 5000°K or more can be reached by laser surface heating. Experiments performed by this technique were reported at the IAEA Thermodynamics Conference (1974, Vienna) by Asami et al /15/, Bober et al /16/, and Ohse et al /17/. The two preliminary data points given by Asami et al, are associated with temperatures measured in the gas phase, and were probably above the critical temperature. However their measurements indicated the possibility of using the technique below the critical point by a reduction of laser pulse length. The vapour pressure data of Bober et al, were not given in form of a vapour pressure curve. The results of Ohse et al, were given in the form of an analytic equation which was suitable for further analysis. Therefore the latter results were used in this work. A somewhat condensed version of the IAEA report by Ohse et al, appears in the preceeding report.

In view of the new experimental information, the equation of state of UO_2 was re-evaluated. In a first step, a critical assessment of the experimental enthalpy and vapour pressure data was carried out, using the fact that these data are connected through the Clausius-Clapeyron equation. For an evaluation of the equation of state up to the critical point, carried out in the second step, it was thought desirable to use a physical model of the liquid state, rather than the principle of corresponding states. The Significant Structure Theory of Eyring (SST) was chosen, since it has successfully predicted the physical properties of a variety of liquids /18/. It has been demonstrated in the literature that both methods reproduce well the equation of state of simple liquids, noble gases and certain molecular liquids. However the SST is believed to be more flexible because it allows, in principle, the consideration of special effects (e.g. ionic bonding, dimerization, electronic excitation, etc.), by modification of the partition function proposed for simple liquids. The principle of corresponding states can be extended by the introduction of a third parameter, the critical compressibility, but the modified form is not very sensitive.

The aim of the present work was to establish the most probable equation of state by checking the consistency of all the data available. The vapour pressure measurements reported in the preceeding report and enthalpy measurements of liquid and solid UO_2 were therefore included in this analysis.

2. Critical Assessment of the Thermodynamic Data for UO_2 Using the Clausius-Clapeyron Equation

The thermodynamic data of solid UO_2 which was used in this work, were enthalpy and vapour pressure measurements.

The experimental enthalpy measurements of Hein et al /8/ and Leibowitz et al /9/ were analyzed by Kerrisk and Clifton /19/. These data, measured up to the melting point, were in good agreement. However, a third set of data of Affortit and Marcon /10/ were not included in the analysis, because they were significantly lower at the melting point.

Vapour pressure data reported in the literature were obtained by two techniques, the effusion method and the transpiration method. Both methods have typical sources of error, which have been discussed elsewhere. In this work, the results of Ohse /7/, consistent with those of Ackermann's High Temperature Experiments /11/ were used as typical of the effusion method, and those of Tetenbaum and Hunt /6/ as representative of the transpiration method. A third "Average Equation" was obtained from all the experimental points available by applying the third law method, and the tabulated free energy functions of Schick /20/.

The analytical fit obtained by Kerrisk and Clifton /19/ for the enthalpy of solid UO_2 in the range 298 to 3133°K is given by the function

$$H_s(t) = \frac{K_1 \Theta}{\exp(\Theta/T)-1} + K_2 T^2 + K_3 \exp(-Ed/RT) \qquad (1)$$

Whereas the assignment of a physical meaning to the first two terms in equation (1), as an Einstein oscillator and an expansion term, may be ambiguous, the third term certainly defines an "excess heat content", which becomes important in the range above 2000°K. It is generally assumed that this excess heat content is due to the formation of Frenkel defects on the oxygen sublattice /21/.

The experimental data for liquid UO_2 used in this assessment were the vapour pressure and heat of fusion, ΔH_f = 17.7 kcal/mol, as reported in the preceeding report. As the experimental points on the vapour pressure of UO_2 cluster around 4600°K, a pressure of 43 atm at 4600°K was taken as the measured value. In addition, C_p of liquid UO_2 near the melting point was measured by Leibowitz et al /12/ as 32.5 cal/mol-K.

The experimental results quoted are connected by the Clausius-Clapeyron Equation, which expresses the vapour pressure dependency on temperature as

$$\frac{dp}{dT} = \frac{H_{sub}}{(V_g - V_c)T}$$

In the range where the volume of the condensed phase, V_c, is negligible compared to V_g, and the vapour can be treated as an ideal gas, this equation may be written

$$\ln \dot{p}\,(T) = \ln p(298) + \int_{298}^{T} \frac{dT}{RT^2} \left[H_g\,(T) - H_c\,(T) + \Delta H_{sub}(298) \right] \qquad (2)$$

For temperatures above the melting point, the integral consists of a contribution from the solid ($H_c = H_s$) and from the liquid ($H_c = H_l$).

The enthalpy of the condensed phase, $H_c(T)$, is given for solid UO_2, by equation (1). For liquid UO_2, it is determined by the heat of fusion and the measured heat capacity C_p, assumed to be constant up to $4600^{\circ}K$. $H_g(T)$ is the enthalpy derived from the usual partition function for a non-linear, polyatomic molecule, which is the product of the translational, rotational and vibrational partition functions

$$f_g = f_g^{\,tr}\, f_g^{\,rot}\, f_g^{\,vib}$$

At present evidence from absorption spectroscopy is given for both non-linear /22/ and linear /23/ molecules. The low frequency line observed by Abramowitz et al /22/ has neither been confirmed nor contradicted. According to Gabelnick et al /23/ the number of peaks and the line intensities depend on both the ratio of partial pressures, being a function of temperature, and on possible impurities, when using different cell materials, such as tungsten and iridium. Under these circumstances it was therefore preferred to use the more general model of a non-linear molecule rather than the special case of a linear molecule.

The expression (2) was used to obtain least-squares fits to the three vapour pressure curves chosen, together with the enthalpy data of Kerrisk and Clifton /19/. In the case of the Ohse measurements, the experimental data points /7/ were used directly for the fit, while in the other cases the vapour pressure equations (Table II) were used. These fits determine $\Delta H_{sub}(298)$ and $\ln p\,(298)$ as parameters. Then by extending the integral in Eq. (2), i.e. extrapolating the vapour pressure curve into
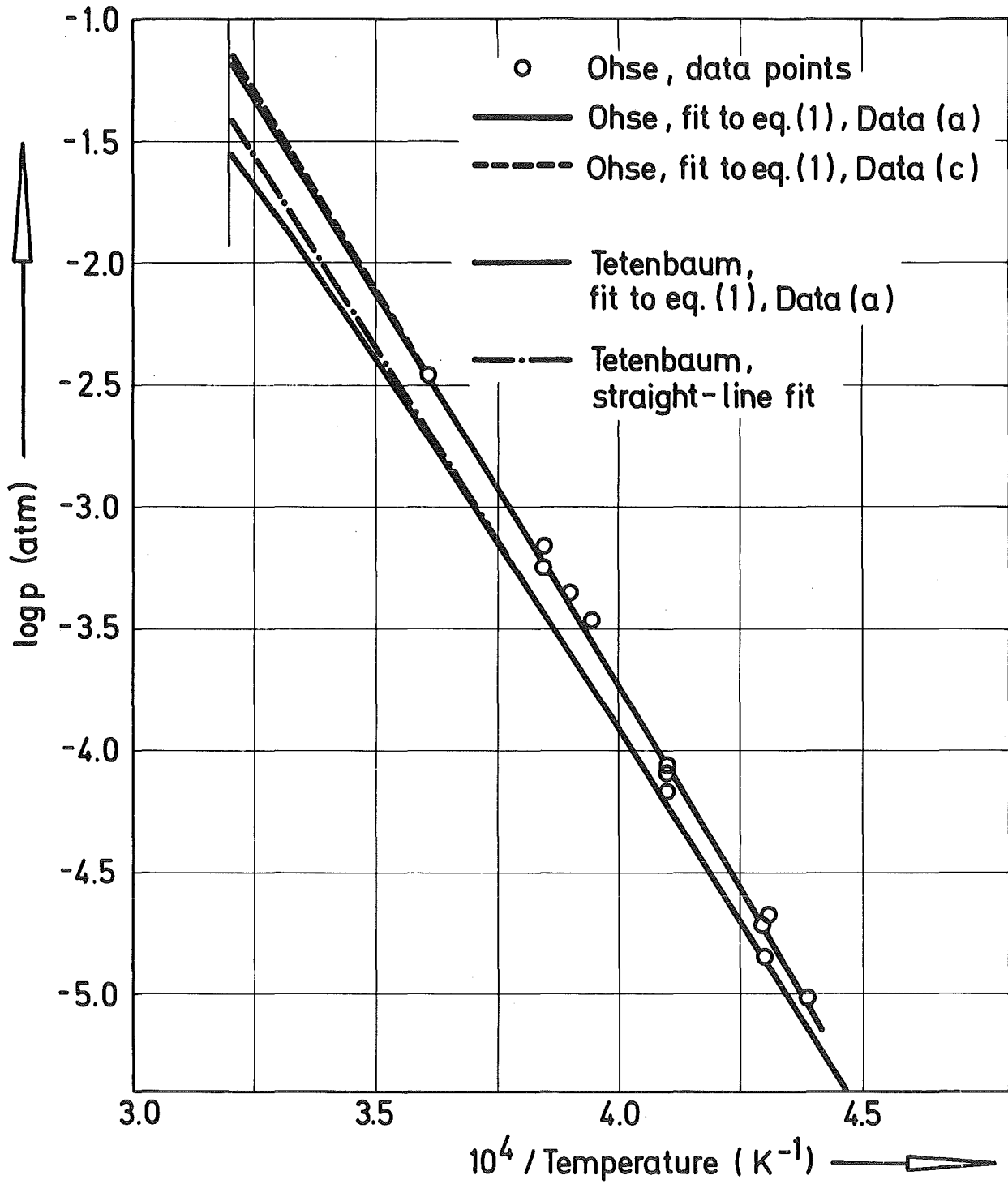
Fig.1 : Vapour Pressure over solid UO₂

Table I   Results of Fits of Vapour Pressure Cur-
___ves to the Clausius-Clapeyron-Equation___

(Melting Point T_m = 3133 K)

Vapour pressure curve	Data	ΔH_{sub} (289)	log p(Tm),atm	ΔH_{sub} (2100-2800)	p(T-4600°K), atm
Ohse	(a)	171.8	- 1.179	151.9	18.1
Averaged curve	(a)	162.2	- 1.366	144.1	8.8
Tetenbaum	(a)	160.8	- 1.545	142.7	4.4
Ohse	(b)	167.4	- 1.162	151.9	25.5
Ohse	(c)	166.8	- 1.151	151.9	28.7
Direct measurement of p (4600°K)					43

Data (a) H_g without electronic excitation

H_s from Kerrisk and Clifton

Data (b) H_g with electronic excitation

H_s from Kerrisk and Clifton

Data (c) H_g with electronic excitation,

H_s weighted average between Kerrisk
and Clifton, and Affortit and Marcon

Table II   Input Data for UO_2

Coefficients of Equation (1) /19/

K_1 19.145 cal/mol-K

K_2 7.847×10^{-4} cal/mol-K^2

K_3 5.644×10^6 cal/mol

K_3 4.515×10^6 cal/mol   (average enthalpy between Kerrisk and Clifton, and Affortit and Marcon)

E_d 37700 cal/mol

Θ 535.28 K

Data of the UO_2 molecule /22/

vibrational frequencies, cm^{-1}

$\nu_1 = 874.2$ $\nu_2 = 79.1$ $\nu_3 = 753.8$

moments of inertia, 10^{-38} g cm^2

$I_1 = 1.33$ $I_2 = 0.64$ $I_3 = 2.14$

electronic partition function (estimated values)

$E_{el} = 8000$ cal/mol $g_0 = 7$ $D = 5 \times 10^{-4}$ mol/cal

Experimental vapour pressure curves

Ohse	log p (atm) = 9.545 - 33183/T	(2200-2800 K)
Tetenbaum	log p (atm) = 8.61 - 31284/T	(2100-2700 K)
Average curve	log p (atm) = 8.846 - 31506/T	(2100-2700 K)

the liquid range, one obtains the pressure p (4600°K), which may be compared to the direct measurement reported in the preceeding report. The results, denoted by "a" are given in Table I, whereas the vapour pressure curve up to the melting point is shown in Fig.1. The values ΔH_{sub} (2100 - 2800), given in the table, are consistent with the slopes of the vapour pressure curves quoted in Table II.

The vapour pressures p (4600°K), as obtained from the extrapolation, are much lower than the experimental value. Considering that equation (2) is derived from thermodynamic principles, and the approximation $V_c << V_g$ is certainly valid in the range considered, one may conclude that there is an inconsistency in the data. The data used in this equation are experimental, except for the enthalpy of the gas. In fact, an important contribution was omitted in the calculation of the enthalpy of the gas, because at the temperatures under consideration, electron excitation certainly gives an additional contribution to the heat capacity. This is evident from an examination of the emission spectrum of thorium /24/ and uranium /25/. However, no measurements exist for the U^{4+} ion, which is present in the UO_2 molecule. Thus, in order to include the heat capacity due to the electronic excitation in the analysis, one has to make an estimate of the distribution of electronic levels in UO_2.

It is felt that it would not be very meaningful to speculate on the position of each electronic level; therefore, the approach taken in this paper is to work with an average level density D(E) per unit energy above a threshold energy. This approach leads to the following expression for the electronic partition function

$$f_g^{el} = g_0 + g_0 \int_{E_e}^{E_i} D(E)e^{-E/RT} dE$$

In this expression, g_0 is the ground state multiplicity, and E_i is the ionization potential. The average level density is assumed constant above the threshold energy E_e. Then, one obtains for the electronic partition function

$$f_g^{el} = g_0(1 + DRTe^{-E_e/RT} - DRTe^{-E_i/RT}) \tag{3}$$

where the last term is small compared to the second one, and may be neglected. Then, the electronic contribution to the internal energy is

$$U_e(T) = \frac{g_0}{f_g^{eT}} \quad DRT \ (E_e + RT) \ e^{-E_e/RT} \qquad (4)$$

In this formalism, the internal energy depends on the two parameters, E_e, and the level density D, which must be estimated. Though any estimates must necessarily have a very large uncertainty, it was found by sensitivity studies that the results do not depend strongly on the values assigned to these parameters. For a reference calculation, the values E_e = 8000 cal/mol, and D = 5×10^{-4} mol/cal were taken. The latter value corresponds about to the average level density of the Th^{2+} ion /24/. In addition, it is necessary to estimate g_0. According to calculations /25/, the ground state of the U^{4+} ion should be a $5f^2$ state. Considering that Th^{2+} has a $5d^2$ ground state with J=2, it is not unreasonable to assume J=3 for U^{4+}, from which follows g_0 = 7.

These parameters were used to repeat some of the fits of vapour pressure data to equation (2) with the improved partition function for gaseous UO_2. In view of the comparison of the pressure values at 4600° K (Table I) the Ohse vapour pressure curve was selected for this further analysis. In an additional case, the enthalpy curve by Kerrisk and Clifton was replaced by a weighted average between the Kerrisk and Clifton fit, and the Affortit and Marcon measurements. This "weighted average H_s" is defined by reducing the parameter K_3 in equation (1) 20% below the value of Kerrisk and Clifton, and corresponds to a reduction of H_s (3000) - H_s(298) by 3 %. The results of these cases are included in Table I. The values p (4600°K) are much closer to the directly measured value, the difference being a factor of 1.5, if "electronic excitation" and "weighted average H_s" is used. This difference should be acceptable, when compared to the normal uncertainties in high temperature vapour pressure measurements.

Thus, the examination of data carried out in this section leads to the following conclusions:

a) Of the pressure values p (4600°K), inferred from the different vapour pressure curves over solid UO_2, only the one based on the effusion data is compatible with the direct measurement. Therefore, the Ohse vapour pressure curve /7/, in good agreement with the Ackermann "high

temperature data" /11/, which are typical of the effusion technique was selected for the further evaluation of the equation of state. Note that this selection is based on the direct measurement of p $(4600^\circ K)$, assuming its reliability.

b) The partition function of gaseous UO_2 at high temperatures should include the contribution from electronic excitation. This is obvious on physical grounds. However, the lack of direct experimental data makes it necessary to use estimated data. Inclusion of this effect brings the value for p $(4600^\circ K)$, extrapolated from lower temperatures, much closer to the measured value, further justifying the inclusion of electronic excitation in the partition function.

c) In order to account for the different measurements of enthalpy for solid UO_2, a "weighted average H_s" between Kerrisk and Clifton, and the Affortit and Marcon measurements was estimated. This "weighted average" again reduces the difference between the p $(4600^\circ K)$ values.

It should be noted that an independent check of data is possible by comparing $\Delta H_{sub}(298)$, as obtained from the Clausius-Clapeyron-Equation ("2nd law values") to the "third law values" obtained from the equation

$$\Delta H^o_{sub}(298) = - T \left[R \ln p + (\frac{G^o(T) - H^o(298)}{T})_{gas} - (\frac{G^o(T) - H^o(298)}{T})_{solid} \right]$$

(5)

Therefore, the free energy functions were re-calculated, in order to introduce recent experimental data. For the solid, expression (1) for the enthalpy, and the relations

$$C_p = \frac{dH}{dT}, \quad S = \int_o^T C_p \, d \ln T, \quad G = H - T S$$

were used.

For the gas, the free energy function was obtained from the partition function. The values calculated on the basis of data "c" (Table I) are listed in Table III.

Table III   Thermodynamic Data for Solid and Gaseous UO_2,

Calculated with Data "c"

Solid UO_2

T, °K	$H^o-H^o(298)$ kcal/mol	C_p^o cal/mol-K	S^o, e.u.	$-(G^o-H(298))/T$, cal/mol-K
300	0.028	15.253	18.504	18.410
400	1.659	17.154	23.183	19.035
500	3.431	18.201	27.133	20.271
600	5.286	18.866	30.515	21.703
700	7.198	19.337	33.460	23.177
800	9.150	19.702	36.067	24.628
900	11.137	20.003	38.405	26.031
1000	13.150	20.264	40.527	27.376
1100	15.189	20.500	42.469	28.661
1200	17.250	20.722	44.263	29.888
1300	19.333	20.940	45.930	31.058
1400	21.438	21.168	47.490	32.177
1500	23.567	21.420	48.959	33.247
1600	25.724	21.716	50.350	34.273
1700	27.913	22.078	51.677	35.258
1800	30.142	22.530	52.952	36.206
1900	32.423	23.096	54.184	37.120
2000	34.766	23.798	55.386	38.003
2100	37.187	24.658	56.568	38.859
2200	39.703	25.691	57.738	39.691
2300	42.332	26.911	58.906	40.501
2400	45.092	28.326	60.080	41.292
2500	48.004	29.941	61.269	42.067
2600	51.087	31.755	62.478	42.829
2700	54.861	33.766	63.713	43.580
2800	57.846	35.964	64.980	44.321
2900	61.560	38.341	66.284	45.056
3000	65.520	40.884	67.626	45.786
3120	70.619	44.135	69.292	46.658

Table III   Thermodynamic Data for Solid and Gaseous UO_2

Calculated with Data "c"

Gaseous UO_2

T, °K	$H^0-H^0(298)$ kcal/mol	C_p^0 cal/mol-K	S^0, e.u.	$-(G^0-H(298)/T$ cal/mol-K
300	0.021	11.192	75.332	75.263
400	1.180	11.863	78.663	75.712
500	2.405	12.516	81.396	76.584
600	3.679	12.935	83.716	77.584
700	4.991	13.296	85.737	78.607
800	6.338	13.646	87.536	79.613
900	7.720	14.004	89.163	80.585
1000	9.139	14.376	90.658	81.519
1100	10.596	14.755	92.046	82.413
1200	12.090	15.132	93.346	83.271
1300	13.622	15.498	94.572	84.093
1400	15.189	15.842	95.733	84.884
1500	16.789	16.158	96.837	85.644
1600	18.419	16.440	97.889	86.377
1700	20.076	16.686	98.893	87.084
1800	21.755	16.894	99.853	87.767
1900	23.454	17.067	100.770	88.427
2000	25.168	17.205	101.650	89.066
2100	26.894	17.313	102.490	89.686
2200	28.629	17.392	103.300	90.286
2300	30.371	17.448	104.070	90.869
2400	32.118	17.482	104.820	91.435
2500	33.867	17.499	105.530	91.985
2600	35.617	17.501	106.220	92.519
2700	37.367	17.492	106.880	93.039
2800	39.115	17.472	107.510	93.544
2900	40.861	17.446	108.130	94.037
3000	42.604	17.413	108.720	94.516
3120	44.691	17.368	109.400	95.076

The "third law values" $\Delta H_{sub}(298)$, were calculated from equation (5) with different data, using the Ohse and Tetenbaum vapour pressure curve. The results are:

Third Law $\Delta H_{sub}(298)$, kcal/mol		
	Ohse	Tetenbaum
Data (a)	155.5	157.4
Data (b)	167.0	168.8
Data (c)	167.1	168.9

The results are practically independent of the vapour pressure data, and can, therefore, only be considered as a check on the free energy function. Inclusion of the electronic partition function brings the heat of sublimation ΔH_{sub}, up by approximately 12 kcal/mol, and though this difference is only estimated, the larger value should be more reliable. It is interesting to note that the second law value is in good agreement with the third law value in this case. It should also be noted that ΔH_{sub} values given in earlier publications are much lower /7/ due to the use of old free energy data.

3. Significant Liquid Structure Theory

3.1 General Outline

The derivation of the equation of state up to the critical point can be carried out using the Principle of Corresponding States, or a model for the liquid state. For reasons given in the introduction, it was decided to use the Significant Structure Theory of liquids (SST) by Eyring /18/, which was very successful in reproducing equation of state data of a number of liquids.

Although originally conceived for simple liquids, it was applied by Eyring and co-workers to other liquids, e.g. molten salts /26 /. A detailed description of the theory is given by Eyring /18/ and will not be repeated in this report. Briefly it is assumed that the liquid is produced from a crystal by taking away molecules from a number of sites and placing them at the edge of the crystal. The "fluid-

ised vacancies" thus produced behave like a gas, whilst the molecules on the remaining lattice sites behave in a solid like manner. Thus the total partition function, f_1, of the liquid is given by the equation

$$f_1(T,V) = f_s^{N \ V_s/V} \ f_g^{N(V-V_s)/V} \tag{6}$$

where f_s and f_g are the partition function of the solid like and gas like molecules, V_s is the volume of the solid at the melting point, and V the volume of the liquid.

The partition function of the gas is given by the product of translational, rotational, vibrational, and electronic partition functions for a non-linear polyatomic molecule

$$f_g = f_g^{tr} \ f_g^{rot} \ f_g^{vib} \ f_g^{el} \tag{7}$$

For f_s the standard form used in the SST /18/ is

$$f_s = \frac{\exp(E_s/RT)}{\left[1-\exp(-\Theta E/T)\right]^3} \left[1 + n \ \frac{(V-V_s)}{V_s} \ \exp(- \frac{a \ E_s \ V_s}{RT(V-V_s)}) \right] \tag{8}$$

with the following notation

E_s = binding energy

Θ_E = Einstein temperature

R = gas constant

a,n = parameters of the model.

The expression (8) contains the partition function for a crystal in the Einstein approximation. The term in brackets accounts for positional degeneracy, which arises because fluidised vacancies provide additional sites for the solid like molecules.

The partition function f_1 is related to the Helmholtz free energy function A, by the equation

$$A \ (T,V) = - \ k \ T \ \ln f_1$$

The other thermodynamic functions can be derived from A in the usual way. In order to obtain the saturation pressure at a given temperature, one has to plot A(T,V) as a function of V, and find the tangent common to two points on the curve, with coordinates V_1 and V_2. V_1 is the volume of the liquid, V_2 that of the saturated vapour, and the slope of the tangent defines the pressure /18/. This procedure is carried out by computer.

3.2 Extrapolation of Excess Enthalpy into the Liquid Range:

Final Form of the Liquid Partition Function of UO_2

The excess heat content of UO_2, described by the third term in equation (1) is assumed to be due to Frenkel defects. In the present work the question arises, how this excess heat content should be treated in the SST. Since there is not sufficient information on the behaviour of defects upon melting, the answer must be sought by arguments based on the principle of the theoretical model.

It is assumed in Eyring's theory that in the liquid the lattice of the crystal still exists, although, it now contains fluidised vacancies occupying some lattice sites. However, the basic properties of the solid like molecules, such as lattice constant, vibrational modes, etc. remain the same as in the solid crystal. It can therefore be argued, that the number of sites for Frenkel defects, and the Frenkel energy should remain unchanged as the material melts. Therefore the defect contribution present in the solid enthalpy should be included in the partition function of the solid like molecules. However, it is obvious that the interaction between defects will become important at higher temperatures, therefore the total defect energy can certainly not increase as rapidly as the direct extrapolation of the heat content in equation (1). In the present report the defect contribution was treated by including the extra factor

$$1 + C_1 \exp(-E_d/RT), \tag{9}$$

per oxygen ion, in the solid like partition function, f_s. The excess heat content and its temperature dependence is then determined by the parameters C_1 and E_d, and they must be chosen such that the ex-
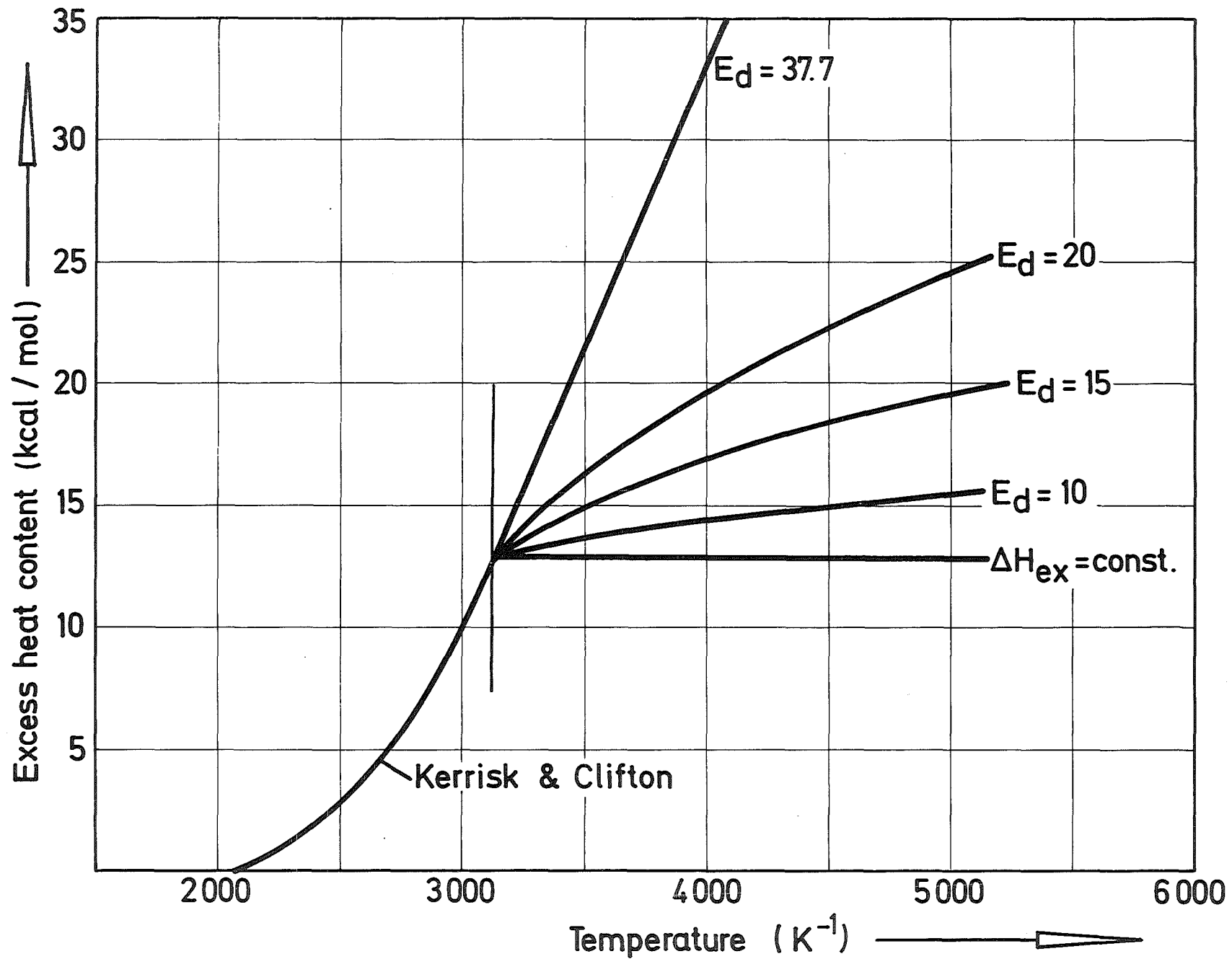
Fig. 2 : Extrapolation of the excess heat content into the liquid range

cess heat content of solid like molecules at the melting point, is the same as that in the solid phase. However, in order to account, in a simplified manner, for the effect of interaction between defects, values of E_d, lower than the one valid for the solid, are proposed, so that the increase in excess heat content with temperature can be reduced (Fig.2). In the limiting case, the excess heat content is constant, and this case can be treated if (9) is replaced by the term $\exp(- \Delta H_{ex}/RT)$.

A parameter study, which was carried out with the different curves of Fig.2, gives the following results:

	C_p	V_1	p $(4600^\circ K)$atm
ΔH_{ex} = const.	34.5	30.84	27.6
E_d = 10 kcal/mol	37.4	30.9	26.7
15 kcal/mol	40.3	30.9	24.6
20 kcal/mol	43.3	30.9	22.6

Considering that the measured value of C_p is 32.5 cal/mol-K /12/ and p(4600K) is 43 atm, it is obvious that the best possible fit is obtained if ΔH_{ex} is taken constant in the liquid phase, thus assuming that the defect concentration is already saturated at the melting point. On the basis of this empirical argument, ΔH_{ex} was assumed constant, without considering the physics of defect interaction in this paper.

Then, the final partition function for solid like UO_2 molecules, as used in this study, is given by the equation

$$f_s = \frac{\exp(\frac{E_s}{3RT}(\frac{V}{V_s})^\gamma - \frac{\Delta H_{ex}}{3RT})}{(1 - e^{-\Theta_E/T})^3} \left[1 + n \left(\frac{V}{V_s} - 1\right)\exp\left(- \frac{a E_s V_s}{3RT(V-V_s)} (\frac{V}{V_s})^\gamma \right) \right] \quad (10)$$

and the partition function for liquid UO_2 is

$$f_1 = f_s^{3N V_s/V} \; f_g^{N(1-V_s/V)} \quad (11)$$

The factor $(V/V_s)^\gamma$, which multiplies E_s in equation (10) was used by Lu et al /26/ in the SST, with $\gamma= 1/3$, to take account of the long-range electrostatic forces in ionic crystals. The behaviour of UO_2 is not expected to be exactly the same as an ionic crystal, therefore, γ was taken as a parameter, rather than set equal to 1/3.

For a molecule as complicated as UO_2, one cannot expect to derive good values for the input parameters of the model from theoretical considerations. Therefore, n, a and γ were adjusted, within a reasonable range of magnitude, such that the vapour pressure at the melting point is that obtained by extrapolating the pressure over the solid range (Table I), and the liquid volume and the heat of fusion are close to the experimental values. Furthermore, also θ_E in equation (9) was obtained from $\Delta H_{sub}(298)$ as given in Table I. The "excess enthalpy" ΔH_{ex} is defined as that part of H_s at the melting point which is in excess of the term described by the Einstein oscillators in equation (10).

3.3 Discussion of Numerical Results Obtained by the SST

As shown in section 2, best agreement between the vapour pressure extrapolated from the measurements over the solid UO_2 /7/ and those measured over liquid UO_2 /17/ was obtained by including the estimated electronic excitation in the gaseous partition function, and using the weighted average enthalpy for the solid UO_2. Therefore, data set "c" was used to obtain the input parameters for the SST, which are shown in Table IV. This table also shows the final results of the calculations. Fig. 3 compares the derived vapour pressure curve to the measured values /17/ and the estimates given by Menzies /3/.

Most of the experimental data at the melting point, namely the specific heat C_p, the molar volume V, the heat of fusion ΔH_f, and the coefficient of thermal expansion α, can be reproduced reasonably well by the model. A discrepancy exists in the case of the compressibility β_T, but only one experimental measurement of β_s/14/ is given in the literature.
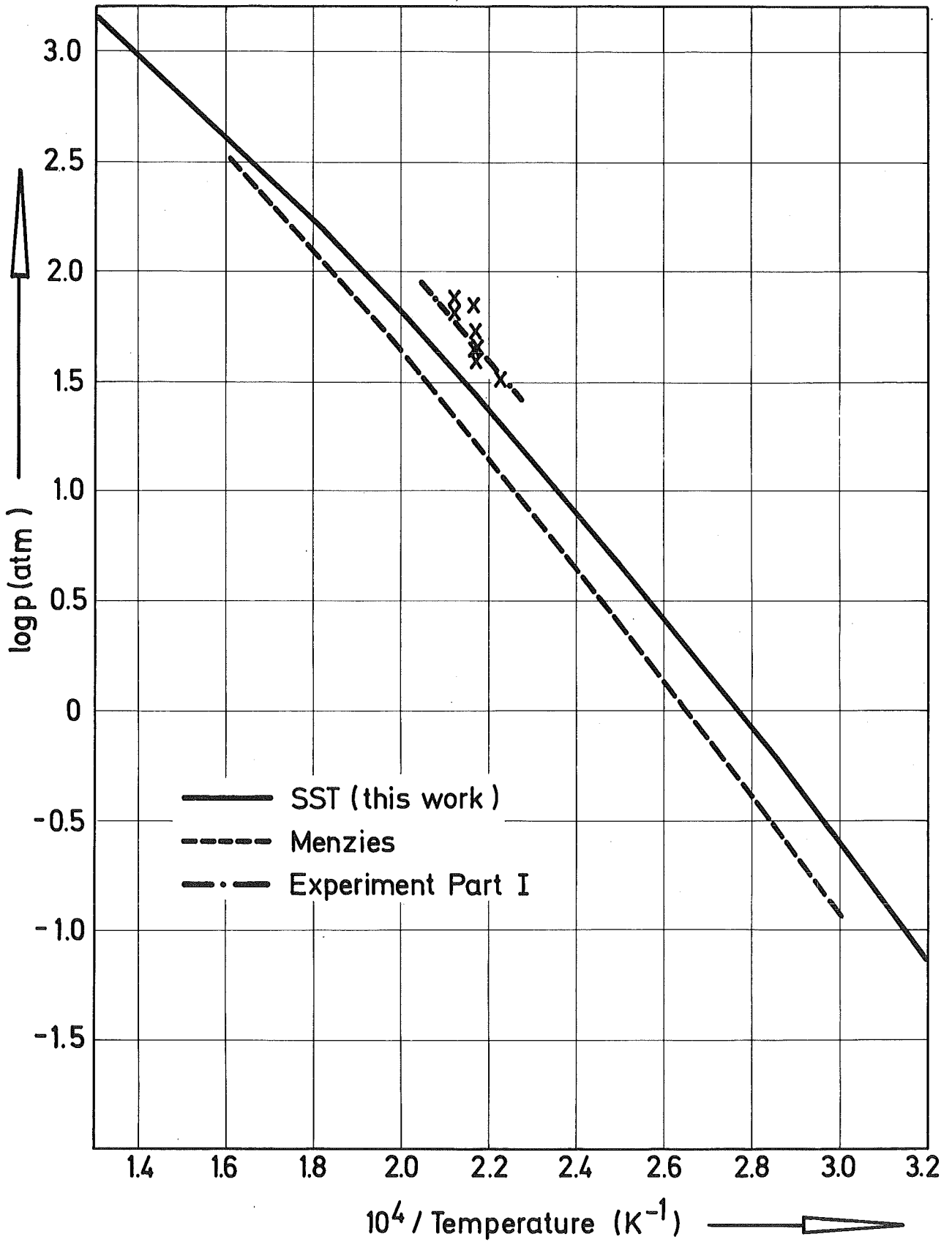
Fig. 3: Vapour Pressure over liquid UO$_2$

Table IV   Input Parameters and Results for the SST Model for UO_2

Input parameters

n	7.2	$\Delta H_{sub}(298)$	166.8 kcal/mol
a	0.0012	E_s	166.6 kcal/mol
γ	-0.10	ΔH_{ex}	19.6 kcal/mol
Θ_E	178 K	V_s	27.9 cm^3/mol

Data at the melting point

	SST	Experiment	Ref. for experim. value
C_p cal/mol-K	34.5	32.5	/12/
V cm^3/mol	30.84	30.9	/13/
ΔH_f, kcal/mol	15.3	17.7	/12/
α, 10^{-4} K^{-1}	1.27	1.05	/13/
β_T, 10^{-12} cm^2/dyn	2.19	$4.4^{a)}$	/14/

a) $\beta_T = \beta_s + \dfrac{VT\alpha^2}{C_p}$, with $\beta_s = 3.6 \times 10^{-12}$ cm^2/dyn /14/

Data at high temperatures

	SST	Experiment
p (4600K), atm	27.6	43
T_c,K	7560	--
P_c, atm	1210	--
ρ_c, g/cm^3	1.66	--
Z_c	0.316	--

The almost identical pressure data p (4600°K) calculated by the SST (Table IV) and the Clausius-Clapeyron-Equation (Table I) with data set "c" are lower than the experimental value /17/ by a factor of about 1.5. The critical temperature is intermediate between several predictions reported in the literature (Table V), and rather close to the value reported by Menzies. On the other hand, the critical pressure and the critical density, are in good agreement with the critical constants by Miller /2/. This agreement should be due to the fact that both evaluations are consistent with the density measurements /13/ by Christensen (Table IV). The critical compressibility Z_c = 0.316, predicted by the SST is consistent with the values accepted in the Principle of Corresponding States.

The critical constants, as derived in this work, have, of course, uncertainties due to inaccuracies in the input data. For the critical temperature, these uncertainties should be of the order of a few hundred degrees. However, the present evaluation is consistent with most of the recent experimental information and therefore, should be considered more reliable than most earlier predictions. The agreement with high-temperature vapour pressure measurements /16,17/ is acceptable.

4. Summary and Conclusions

Since Meyer and Wolfe /1/, Miller /2/, and Menzies /3/ derived equation of state data for UO_2 from the principle of corresponding states, additional thermodynamic data have become available from experimental measurements. In particular, vapour pressure studies over liquid UO_2 up to 5000°K (preceeding report) and enthalpy measurements for solid UO_2 up to the melting point have been carried out. In view of this new information, the equation of state for UO_2 was re-evaluated.

A critical assessment of the experimental data was carried out using the Clausius-Clapeyron-Equation. In order to obtain agreement between the reported vapour pressure measurements over solid UO_2 and the recent pressure measurements over liquid UO_2, it was necessary to consider effusion measurements only, and to include an electronic excitation term in the gaseous partition function. From this a new set of free energy functions was calculated for gaseous and solid UO_2. On the basis of this set of

Table V   Comparison of Critical Constants for UO_2 Evaluated

by Different Authors

		T_c, K	p_c, atm	ρ_c, g/cm^3	Remarks
Meyer and Wolfe /1/	A	8000	1980	3.01	
Menzies /3/	A	7300	1900	3.16	
Miller /2/	B	9110	1230	1.59	Average values within a range of parameter variations
Gillan /5/	C	6960	1070	1.64	based on Ohse's vapour pressure data /7/
Gillan /5/	C	9330	1450	1.63	based on Tetenbaum's vapour pressure data /6/
This work	C	7560	1210	1.66	based on Ohse's vapour pressure data /7/

A   Principle of Corresponding States

B   Method of Rectilinear Diameter

C   Significant Structure Theory

thermodynamic data, a new equation of state for UO_2 was derived from the significant structure theory of liquids, which is in good agreement with the recent vapour pressure data over liquid UO_2.

In addition, this equation is consistent with data for the specific heat, the molar volume, and the thermal expansion coefficient for liquid UO_2 at the melting point, whereas a discrepancy exists in the case of the isothermal compressibility. The critical constants obtained are $T_c = 7560^{\circ}$K, $p_c = 1210$ atm and $\rho_c = 1.66$ g/cm^3; the critical compressibility $p_c V_c / RT_c = 0.316$, compares well with the values predicted by the theory of corresponding states.

REFERENCES

/1/   R.A. Meyer and B.E. Wolfe, Report GEAP-4809

/2/   D. Miller, Conference on Safety, Fuels and Core Design in Large Fast Power Reactors, ANL-7120, (1965) 641

/3/   C. Menzies, UKAEA Report TRG-1119 (D) (1966)

/4/   D.L. Booth, UKAEA Report TRG-1759 (R/X) (1968), reprinted 1974

/5/   M.J. Gillan, Derivation of an Equation of State for Liquid UO_2 Using the Theory of Significant Structures, IAEA-Conference on Thermodynamics of Nuclear Materials, Vienna, Oct. 1974

/6/   M. Tetenbaum and P.D. Hunt, J.Nucl.Mater. $\underline{34}$ (1970) 86

/7/   R.W. Ohse, Euratom Report EUR 2166 e (1964) and J.Chem.Phys. 44 (1966) 1375

/8/   R.A. Hein, L.H. Sjodahl, and R. Szwarc, J.Nucl.Mater. 25 (1968) 99

/9/   L. Leibowitz, L.W. Mishler and M.G. Chasanov: J.Nucl.Mater. 29 (1969) 356

/10/   C. Affortit and J. Marcon, Rev. Int. Hautes Tempér. et Refract. 7 (1970) 236

/11/   R.J. Ackermann, P.W. Gilles and R.J. Thorn, J.Chem.Phys. 25 (1956) 1089, see also report ANL-5482 (1955)

/12/   L. Leibowitz, M.G. Chasanov, L.W. Mishler, D.F. Fischer, J.Nucl. Mater. 39 (1971) 115

/13/   J.A. Christensen, J.Amer.Ceram.Soc. 46 (1963) 607

/14/   O.D. Slagle and R.P. Nelson, J.Nucl. Mater. 40 (1971) 349

/15/   N. Asami, N. Nishikawa and M. Taguchi, Experimental Investigation of Ultra-High Temperature and Pressure State of Uranium Dioxide, IAEA Conference on Thermodynamics of Nuclear Materials, Vienna Oct. 1974

/16/   M. Bober, H.U. Karow, K. Schretzmann, Evaporation Experiments for the Determination of the Vapour Pressure of UO_2 Fuel in the Temperature Range from 3000 to 5000 K, ibid. (1974)

/17/   R.W. Ohse, P.G. Berrie, H.G. Bogensberger, E.A. Fischer, Contribution of Uranium Plutonium Oxide Pressure, and Influence of Radial Fission Product Distribution on Pin Failure of Fast Breeder Fuels under Accident Conditions, ibid. (1974)

/18/ H. Eyring, M.S. Jhon, Significant Liquid Structures,
      Wiley, New York (1969)

/19/ J.F. Kerrisk and D.G. Clifton, Nuclear Technology 16 (1972) 531

/20/ H. Schick, Thermodynamics of Certain Refractory Compounds,
      Academic Press (1966)

/21/ B.T.M. Willis, Le Journal de Physique 25 (1964) 431

/22/ S. Abromawitz, N. Acquista and K.R. Thompson, J.Phys.Chem. 75
      (1971) 2283 and 76 (1972) 648

/23/ S.D. Gabelnick, G.T. Reedy and M.G. Chasanov, J.Chem.Phys. 58
      (1973) 4468

/24/ G.W. Charles, USAEC Report ORNL-2319 (1958)

/25/ D.W. Steinhaus et al., USAEC Report LA-4501 (1971)

/26/ W.C. Lu, T. Ree, V.G. Gerrard, H. Eyring, J.Chem.Phys. 49
      (1968) 797